University of Reading

COMPRESSIBLE FLOW IN DUCTS - AN ADAPTIVE GRID METHOD

J. R. WIXCEY

NUMERICAL ANALYSIS REPORT 14/88

DEPARTMENT
OF MATHEMATICS

COMPRESSIBLE FLOW IN DUCTS - AN ADAPTIVE GRID METHOD

J. R. WIXCEY

NUMERICAL ANALYSIS REPORT 14/88

Department of Mathematics
P.O. Box 220
University of Reading
Whiteknights
Reading
RG6 2AX
United Kingdom

This work forms part of the research programme of the Institute of Computational Fluid Dynamics at the Universities of Oxford and Reading and has been supported by the S.E.R.C.

CONTENTS

ABSTRACT

In this report we derive, from a stationary principle, a local finite element method on an adaptive grid for the approximate solution of quasi one-dimensional duct flow. A solution algorithm is then presented. The method, together with various associated treatments, is applied to the approximate solution of two particular duct motions. Numerical and graphical results for each are presented and comparison made with the numerical solution in [2] of the same motions on a fixed uniform grid.

ACKNOWLEDGEMENTS

I am grateful to Dr. M.J. Baines and Dr. D. Porter for their continuous encouragement and guidance during this work.

I acknowledge an S.E.R.C. research studentship.

INTRODUCTION

This is the third report of a series in which we discuss the exact and approximate solution of duct flow. In the first report a quasi one-dimensional approximation to duct flow was presented [1] and this was used to obtain an algebraic parameterisation of the flow. In the second report a stationary principle representative of quasi one-dimensional duct flow was constructed [2] and used to derive a finite element method on a fixed grid for the approximate solution of the flow. By using the algebraic parameterisation as a comparative exact solution it was concluded that a numerical method is required that will still be accurate when there is significant curvature in the solution. The aim of this third report is the derivation of a finite element method on an adaptive grid from the same stationary principle.

The stationary principle representative of quasi one-dimensional duct flow is stated in Section One and the adaptive grid finite element method then formulated.

In Section Two the resulting system of equations is recast in a local manner and the basic solution algorithm presented.

In Section Three the method is applied to the approximate solution of a particular converging cone section flow; this includes the discussion of the occurrence of singularity of the local system of equations. The results obtained are compared to the approximate solution for the same motion on a fixed uniform grid, as found in [2].

In Section Four the adaptive grid method is applied to the approximate solution of flow through a de-Laval nozzle; two alternative treatments of the node at the nozzle throat are considered. The results are compared with each other and also with the equivalent fixed grid solution found in [2].

SECTION ONE : A NUMERICAL FORMULATION OF QUASI ONE-DIMENSIONAL DUCT FLOW ON AN ADAPTIVE GRID

In this section a finite element method on an adaptive grid is formulated from a stationary principle for the approximate solution of duct flow.

The compressible fluid to be considered is modelled by the polytropic gas with the appropriate equation of state

$$p = \eta \rho^{\gamma} , \tag{1.1}$$

where p represents the pressure, ρ the density, and γ is the adiabatic exponent associated with the fluid medium. The conservation equations of fluid dynamics governing the fluid motion in quasi one-dimensional duct flow are (see [2])

$$\text{CONSERVATION OF MOMENTUM} : h = \text{CONSTANT} , \tag{1.2}$$

where h is the constant total energy in the homenergic flow,

$$\text{CONSERVATION OF ENERGY} : \eta = \text{CONSTANT} , \tag{1.3}$$

where $\eta = \eta(S)$ is the constant function of entropy, S, in the homentropic flow, except at discontinuities, and

$$\text{CONSERVATION OF MASS} : \frac{d}{dx}(Q A) = 0 , \tag{1.4}$$

where A = A(x) is the cross-sectional area of the duct and Q = Q(x) is the local mass flow rate defined by

$$Q = \rho v. \tag{1.5}$$

where v represents the fluid speed. The complete solution of the flow, in which all of the flow variables are recovered, is possible on using the total energy equation in its appropriate form

$$h = \aleph(\rho, \eta) + (v^2/2) , \tag{1.6}$$

where $\aleph$ is the enthalpy.

The particular fluid flow to be considered is that of air, defined by the associated thermodynamic constants

$$\gamma = 1.4 ,$$
$$R_o = 8.31 \text{ Jmol}^{-1}\text{K}^{-1} \tag{1.7}$$
and $$m = 28.96 \times 10^{-2} \text{ Kg} ,$$

where R_o is the universal gas constant and m is the molecular weight of the gas, together with the flow constants

$$h = 2.74 \times 10^5 \text{ Jmol}^{-1}\text{K}^{-1}$$
and (1.8)
$$\eta = 7.08 \times 10^4 \text{ (SI UNITS)} ,$$

(as used in [1] and [2]).

The defining equations (1.2) - (1.5) are considered to hold in a

fixed domain, D, representing the duct axis. In order to be able to solve a particular duct flow mass conservation is ensured by assigning

$$Q(x)\ A(x) = \text{CONSTANT} \ . \tag{1.9}$$

which is chosen (see [1]) such that

$$Q(x) = \frac{C\ A_e}{A(x)} \ , \tag{1.10}$$

where C is the mass flow entry value corresponding to the central streamline along the duct axis and A_e is the duct entry cross-sectional area.

A stationary principle representative of quasi one-dimensional duct flow has been postulated in [2], namely

$$\delta I = \delta \left[\int_D \left(\frac{C\ A_e}{A(x)}\ v + p(v) \right) dx \right] = 0 \ . \tag{1.11}$$

The stationary principle (1.11) has been used in [2] to derive a finite element method on a fixed grid for a piece-wise linear approximation to the fluid speed throughout the duct, with respect to the distance, x, along the duct axis.

A method is now formulated on an adaptive grid in which not only are the nodal amplitudes $a_i = a_i(k)$, $i = 1(1)N$, unknown at each iteration level, k, towards the final approximate solution, but additionally the corresponding nodal positions $s_i = s_i(k)$, $i = 1(1)N$, are not known. A semi-discrete solution of the form

$$\bar{v}(x,k) = \sum_{i=1}^{N} a_i(k)\ \alpha_i(x,\underline{s}(k)) \qquad (1.12)$$

in a sub-space of C^o is sought, where $\alpha_i = \alpha_i(x,\underline{s}(k))$, i = 1(1)N, are piece-wise linear basis functions with local compact support and $s(\underline{k})$ is the vector of nodal positions; an interior 'α-type' basis function is shown in FIG.1 and defined by

$$\alpha_i = \begin{cases} \dfrac{x - s_{i-1}}{s_i - s_{i-1}} & s_{i-1} \le x \le s_i \\ \dfrac{s_{i+1} - x}{s_{i+1} - s_i} & s_i \le x \le s_{i+1} \end{cases} \qquad [\ i = 2(1)N-1\ ]\ , \quad (1.13)$$

α_i being zero outside the interval $[\ s_{i-1}\ ,\ s_{i+1}\ ]$.

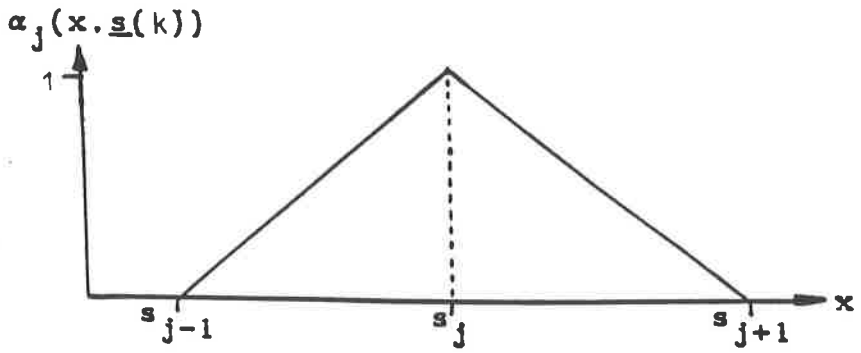

FIG.1

The substitution of the approximation to the fluid speed (1.12) into the functional, I, underlying the stationary principle (1.11), yields now a function, L, of the unknown coefficients a_i and s_i

$$L = L(\ a_1,\ s_1,\ a_2,\ s_2,\ \ldots\ ,\ a_{N-1},\ s_{N-1},\ a_N,\ s_N\ )\ , \qquad (1.14)$$

where $L = I(\bar{v})$ is defined by

$$L = \int_D \left[\frac{C A_e}{A(x)} \bar{v} + p(\bar{v}) \right] dx \ , \qquad (1.15)$$

on the same domain, D, as its counterpart in continuous space. Therefore making the function (1.15) stationary gives an approximation to the stationary point of the functional I in the chosen subspace; the conditions for this are simply

$$\frac{\partial L}{\partial a_i} = 0 \qquad [\ i = 1(1)N\ ]$$

and (1.16)

$$\frac{\partial L}{\partial s_i} = 0 \ . \qquad [\ i = 1(1)N\ ]$$

The partial derivative (1.16) may be written explicitly

$$\int_D \left[\frac{C A_e}{A(x)} - \rho \bar{v} \right] \alpha_i \, dx = 0 \ , \qquad [\ i = 1(1)N\ ] \qquad (1.18)$$

using (see [2])

$$p'(\bar{v}) = - \rho \bar{v} \ . \qquad (1.19)$$

Similarly (1.17) may be written

$$\int_D \left[\frac{C A_e}{A(x)} - \rho \bar{v} \right] \beta_i \, dx = 0 \ , \qquad [\ i = 1(1)N\ ] \qquad (1.20)$$

using (see [3])

$$\frac{\partial \bar{v}}{\partial s_i} = \beta_i \ , \tag{1.21}$$

with $\beta_i = \beta_i(x, \underline{a}(k), \underline{s}(k))$ a second type of basis function with the same local compact support as α_i, $a(\underline{k})$ being the vector of unknown nodal amplitudes, such that

$$\beta_i = \begin{cases} - m_{i-1}\ \alpha_i & s_{i-1} \leq x \leq s_i \\ \\ - m_i\ \alpha_i & s_i \leq x \leq s_{i+1} \ , \end{cases} \tag{1.22}$$

where

$$m_i = \frac{a_{i+1} - a_i}{s_{i+1} - s_i} \ , \tag{1.23}$$

can be interpreted as the slope of the approximate solution, $\bar{v}$, in the open interval (s_i , s_{i+1}); a typical 'β-type' basis function is shown in FIG.2.

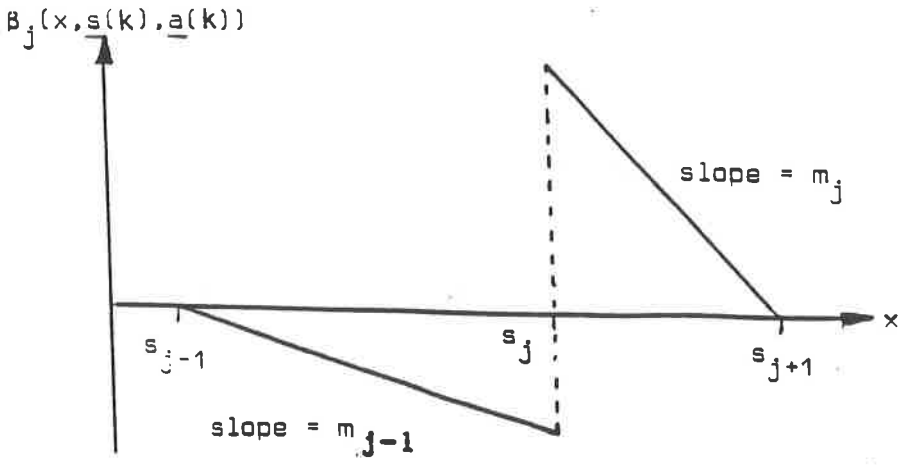

FIG TWO

The conditions (1.18) and (1.20) now take the form of a system of equations at each iteration level for the unknown parameters $\underline{a}(k)$ and $\underline{s}(k)$ and. the aim being to derive the approximate fluid speed variation throughout the duct, the density term in these equations is replaced by the algebraic relation (see [4])

$$\rho(\bar{v}) = \eta^{(1/1-\gamma)} \left[(\gamma-1/\gamma) (h - (\bar{v}^2/2)) \right]^{(1/\gamma-1)}, \qquad (1.24)$$

The conditions (1.18) and (1.20) may then be written in terms of the inner product

$$\langle \phi , \psi \rangle = \int_D \phi \psi \, dx , \qquad (1.25)$$

as

$$\begin{aligned} &\left\langle \frac{C A_e}{A(x)} - \rho(\bar{v}) \bar{v} , \alpha_i \right\rangle = 0 \\ &\qquad\qquad [i = 1(1)N] \qquad (1.26) \\ &\left\langle \frac{C A_e}{A(x)} - \rho(\bar{v}) \bar{v} , \beta_i \right\rangle = 0 , \end{aligned}$$

where $\langle \cdot, \cdot \rangle$ denotes integration over the domain, D, which it may be noted from (1.10) are simply weak forms of (1.5).

On solution of the system (1.26) the function (1.15) has been made stationary with respect to its arguments, solving the given flow problem discretely, and thus determining an approximation to the axial fluid speed variation in the motion.

SECTION TWO : THE SOLUTION OF THE EQUATION SYSTEM

An algorithm is required for the solution of the non-linear equation system (1.26). In the numerical solution of duct flow on a fixed grid (see [2]) Newton's method for several variables is employed to solve for the unknown amplitude parameters a_i, i = 1(1)N. This algorithm may be extended to solve the present system, including now the unknown nodal positions, i.e. the numerical grid, at each iteration level. After considerable work with this algorithm, including various modifications, it was concluded that the Jacobian matrix of the equation system (1.26) is often extremely ill-conditioned, and consequently an alternative approach is required. The basic solution algorithm that has been implemented is outlined in this section. The discussion of more detailed features will take place where appropriate in subsequent sections of the report.

2.1 THE BASIC SOLUTION ALGORITHM

The solution domain representing the duct axis is defined to be

$$0.0 \leq x \leq d \ , \qquad (2.1)$$

where d is the domain length. The statement of the solution algorithm is now made in two stages.

1. The fixed grid solution stage

A piece-wise linear approximation to the fluid speed variation throughout a duct is first obtained on a fixed grid: the full formulation may be found in [2], but a brief outline is presented here stating the factors necessary for progression to the adaptive grid stage.

A fixed numerical grid consisting of N nodes, denoted by $\underline{s}_F$, is specified such that nodes are placed at the domain extremes, i.e.

$$s_1 = 0.0 \ , \qquad (2.2)$$
$$s_N = d \ ,$$

and the remaining interior nodes are uniformly spaced

$$s_i = (i - 1)(d/N) \qquad [\ i = 2(1)N-1\ ] \ . \qquad (2.3)$$

The equation system $f_i(\underline{a}) = 0$, $i = 1(1)N$, for the unknown nodal amplitudes a_i, $i = 1(1)N$, at each iteration level on the fixed grid, is then solved by Newton's method; the iteration is said to have converged when the maximum absolute point-wise residual error of the equation system is less than a specified tolerance, here taken to be

$$\text{MAX} \ | \ f_i(\underline{a}) \ | \ < 0.00001 \qquad [\ i = 1(1)N\ ]. \qquad (2.4)$$

The resulting solution vector, $\underline{a}_F^*$, is now used, together with the corresponding nodal positions defined by (2.2) and (2.3), to form the initial data vector, $\underline{w}_A^o$, for the adaptive grid stage, where

$$\underline{w}_A^o = (\underline{a}_F^* , \underline{s}_F) = (a_1^*, s_1, a_2^*, s_2, \ldots , a_N^*, s_N) . \qquad (2.5)$$

Hence, prior to any displacement of the nodes, the initial data vector (2.5) will contain approximately the correct solution curvature, which should mimimise the appearence of ill-conditioning in the adaptive grid solution procedure.

2. The adaptive grid solution stage

The possibly ill-conditioned nature of the Jacobian of the equation system may be controlled by updating the nodes individually in a local manner [5], the basic steps of which are now presented.

(a) The nodes at the domain extremes (2.2) are constrained to move in amplitude only. These nodes are the first to be updated by solving the associated equations

$$F_i^k \equiv \langle \frac{C\, A_e}{A(x)} - \rho \bar{v} , \alpha_i \rangle = 0 , \qquad [i = 1, i = N] \qquad (2.6)$$

using the simple single variable Newton method

$$a_i(k+1) = a_i(k) - \left[F_i^k \Big/ \left[\frac{dF_i}{da_i} \right]^k \right] . \qquad (2.7)$$

Prior to updating the interior nodes in the solution domain the equation system is recast in a manner reflecting the local nature of the formulation. The form of the β-type basis function (see (1.22) and FIG.2) allows the definition, here in a node-wise manner, of an

alternative set of local basis functions $\phi_{iL} = \phi_{iL}(x,\underline{s}(k))$, $i = 2(1)N-1$, and $\phi_{iR} = \phi_{iR}(x,\underline{s}(k))$, $i = 2(1)N-1$, (see [3])

$$\phi_{iL} = \frac{x - s_{i-1}}{s_i - s_{i-1}} \qquad s_{i-1} \leq x \leq s_i$$

$$[\ i = 2(1)N-1\ ] \qquad (2.8)$$

$$\phi_{iR} = \frac{s_{i+1} - x}{s_{i+1} - s_i} \qquad s_i \leq x \leq s_{i+1}\ ,$$

ϕ_{iL} and ϕ_{iR} being zero elsewhere (see FIG.3), as a linear combination of α_i and β_i such that

$$\begin{bmatrix} \alpha_i \\ \beta_i \end{bmatrix} = \begin{bmatrix} 1 & 1 \\ -m_{i-1} & -m_i \end{bmatrix} \begin{bmatrix} \phi_{iL} \\ \phi_{iR} \end{bmatrix}, \qquad [\ i = 2(1)N-1\ ] \qquad (2.9)$$

where m_{i-1} and m_i are the local approximate gradients of the solution defined by (1.23).

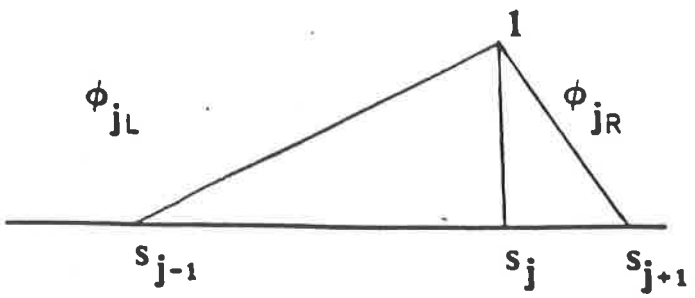

FIG THREE

Providing that $m_{i-1} \neq m_i$, the system of equations corresponding to the interior nodes may then be written as 2 x 2 non-overlapping pairs

$$\underline{F}_i^k = \begin{cases} F_{iL}^k \equiv \left\langle \dfrac{C\,A_e}{A(x)} - \rho\,\bar{v}\,,\ \varphi_{iL} \right\rangle = 0 \\ \qquad\qquad [\ i = 2(1)N-1\ ] \\ F_{iR}^k \equiv \left\langle \dfrac{C\,A_e}{A(x)} - \rho\,\bar{v}\,,\ \varphi_{iR} \right\rangle = 0\ , \end{cases} \tag{2.10}$$

and the interior nodes may now be updated in the following manner.

(b) The present solution vector, $\underline{w}^k$, is fixed except for the amplitude, a_i, and position, s_i, of the particular node under consideration.

(c) The parameters a_i and s_i are updated by solving the local system of equations associated with this node by a two variable form of Newton's method

$$\underbrace{\begin{bmatrix} A & B \\ C & D \end{bmatrix}}_{[J]_i^k} \underbrace{\begin{bmatrix} \delta a_i^k \\ \delta s_i^k \end{bmatrix}}_{\delta \underline{w}_i^k} = - \underbrace{\begin{bmatrix} F_{iL}^k \\ F_{iR}^k \end{bmatrix}}_{\underline{F}_i^k}\ , \tag{2.11}$$

where the vector of local parameter updates, $\delta \underline{w}_i^k$, consists of the update in amplitude, δa_i^k, and in position, δs_i^k, and the elements of the local Jacobian matrix, $[J]_i^k$, are

$$A = \frac{\partial F_{iL}^k}{\partial a_i^k}\ ,\ B = \frac{\partial F_{iL}^k}{\partial s_i^k}\ ,\ C = \frac{\partial F_{iR}^k}{\partial a_i^k}\ ,\ D = \frac{\partial F_{iR}^k}{\partial s_i^k}\ , \tag{2.12}$$

where note that δ is used here in a totally different sense to that of variations in Section One. The local system (2.11) is solved

simultaneously to give

$$\delta s_i^k = \frac{1.0}{D - (B\ C/A)} \left[- F_{iR}^k + \left[\frac{C}{A} F_{iL}^k \right] \right] \qquad (2.13)$$

and by back substitution

$$\delta a_i^k = \frac{1.0}{A} \left[- F_{iL}^k + \delta s_i^k\ B \right] , \qquad (2.14)$$

(assuming $D \neq B\ C/A$) whence the parameters a_i and s_i may be updated according to

$$a_i^{k+1} = a_i^k + \delta a_i^k$$

and $$\qquad (2.15)$$

$$s_i^{k+1} = s_i^k + \delta s_i^k .$$

(d) Note that this procedure will redefine the neighbouring local basis functions and thus the corresponding equations in the system (2.10), i.e.

$$\left\langle \frac{C\ A_e}{A(x)} - \rho\ \bar{v}\ ,\ \phi_{i-1R} \right\rangle = 0$$

and $$\qquad (2.16)$$

$$\left\langle \frac{C\ A_e}{A(x)} - \rho\ \bar{v}\ ,\ \phi_{i+1L} \right\rangle = 0 .$$

(e) The algorithm then proceeds to update each of the interior nodes once both in amplitude and position by setting $i = i + 1$ and returning to stage (b).

It may then be said that, including the updating of the boundary

nodes. N local iterations (one 'sweep') have been performed. The adaptive grid stage of the solution is said to have converged to the final approximate solution vector when the maximum absolute nodal displacement update for a complete sweep is less than the specified tolerance

$$\text{MAX} \mid \delta s_i \mid < 0.0001 \qquad [\ i = 2(1)N-1\ ]\ . \tag{2.17}$$

It is of course possible to update each node in turn more than once before progressing to the next node, or even to iterate to convergence of each local system (2.11). The principle behind the basic algorithm though is that the nodes neighbouring that being updated are temporarily assumed to be at the exact solution, which is of course not the case until the final sweep, and thus acting in the above manner is expensive and most probably unnecessary. This point is dealt with in more detail later (see §4.5).

2.2 AN ALGORITHM MODIFICATION

In the basic algorithm (§2.1) the interior nodes are updated in the natural ordering, i.e. i = 2(1)N-1. However, owing to the local nature of the solution algorithm, the interior nodes may be updated in any order and a particularly efficient ordering algorithm results on consideration of the local element gradients at each node.

(a) Subsequent to having updated the amplitudes of the boundary nodes, the maximum absolute element gradient, M_i, where

$$M_i = \text{MAX} \mid m_{i-1}\ ,\ m_i \mid \qquad [\ i = 2(1)N-1\ ]\ , \tag{2.19}$$

associated with each interior node is computed.

(b) The gradients (2.19) are then sorted into descending magnitude, keeping associated with each the respective node number, and the interior nodes are then updated in the resulting order.

(c) The use of this ordering will theoretically induce more nodal movement per sweep, and thus a faster convergence rate to the final solution vector and ultimately a more efficient solution algorithm.

The system solution algorithm is now applied to find the numerical solution, on an adaptive grid, of two particular duct motions.

SECTION THREE : THE ADAPTIVE GRID SOLUTION OF CONE SECTION FLOW

The adaptive grid formulation is now applied to the approximate solution of the flow through a converging cone section. The results obtained are compared with the approximate solution of the same motion on a uniform fixed grid (see [2]).

3.1 DEFINITION OF MOTION

The domain on which the cone section lies is defined as

$$0.0 \leq x \leq 1.0 \ , \tag{3.1}$$

and the particular converging cone section flow is specified by the area variation

$$A(x) = 1 + 0.1\ (1-x) + 0.05\ (1-x)^2 \ , \tag{3.2}$$

such that

$$A_e = 1.15$$

and $$A_o = 1.0 \ ,$$

where A_o is the outlet cross-sectional area, together with the mass flow boundary condition at inlet (see [2])

$$C = 200.0 \tag{3.3}$$

and at outlet

$$Q_o = 230.0 \ .$$

The associated stationary principle for this motion is obtained by substitution of (3.2ab) and (3.3a) into (1.11),

$$\delta\Big[\int_D \Big[\frac{230.0\ v}{1 + 0.1(1-x) + 0.05(1-x)^2} + p(v) \Big]\ dx \Big] = 0 \ . \qquad (3.4)$$

3.2 THE IMPLEMENTATION OF THE SYSTEM SOLUTION ALGORITHM

The approximate fluid speed variation throughout the cone section is now obtained in two stages, as described in §2.1. The problem is first solved on a fixed grid, defined by (2.2) and (2.3), where note from (3.1) the domain length is 1.0.

There will exist two independent solution vectors on the fixed grid corresponding to the possibility of one of either subsonic, $\underline{a}^*_{Fsub}$, or supersonic, $\underline{a}^*_{Fsup}$, flow throughout the cone section (see [1] and [2]). The constant initial data vector, $\underline{a}^o_F$, is specified in accordance with the initial data regions derived in [2] so as to obtain the approximate solution to both of these flow types

$$\text{SUBSONIC FLOW} \quad : \quad \underline{a}^o_F = 200.0$$

and (3.5)

$$\text{SUPERSONIC FLOW} \quad : \quad \underline{a}^o_F = 500.0 \ .$$

The piece-wise linear approximation to the fluid speed in subsonic flow , using 7 nodes, on the fixed grid is shown in FIG.4*ii* and in supersonic flow, when using 10 nodes, in FIG.4*iv*. The corresponding solution vectors, $\underline{a}^*_{Fsub}$ and $\underline{a}^*_{Fsup}$, may now be used in turn in the initial data vector, $\underline{w}^o_A$, for the adaptive grid solution stage

$$\text{SUBSONIC FLOW} \quad : \quad \underline{w}_A^o = (\underline{a}^*_{Fsub} , \underline{s}_F) \qquad (3.6)$$

$$\text{SUPERSONIC FLOW} \quad : \quad \underline{w}_A^o = (\underline{a}^*_{Fsup} , \underline{s}_F) .$$

so as to obtain the adaptive grid solution vector for subsonic flow, $\underline{a}^*_{Asub}$, and for supersonic flow, $\underline{a}^*_{Asup}$.

3.3 SINGULARITY OF THE LOCAL SYSTEM

We now consider the case when the Jacobian, $[J]_i^k$, of the local system (2.11) becomes singular, i.e. A D = B C, in the adaptive grid stage. A situation in which this may be expected to occur is on occurrence of parallelism in the piece-wise linear solution, i.e. when adjacent element slopes become equal or a when a node and its two neighbours are collinear, namely

$$\text{AT NODE } i \quad : \quad m_{i-1} = m_i . \qquad (3.7)$$

This will actually correspond in the present case to there being a linear region in the exact solution; close to collinearity the local Jacobian becomes nearly singular and as a result the 'parallel node' migrates very rapidly towards one of its neighbouring nodes. Singularity will also occur if co-incidence of two nodes takes place, and again this is found when the determinant of $[J]_i^k$ is zero

$$\det [J]_i^k \equiv A\ D - B\ C = 0 . \qquad (3.8)$$

The treatment of a 'parallel node' is now discussed. As stated above the rapid migration is a consequence of the discrete solution

being unable to uniquely represent a linearity present in the solution. As a result of this movement merging of nodes may occur, but the replacement of one of these nodes into a suitable location in the solution domain (by conservation of area, or similar arguments) would appear unfounded and unnecessary. Therefore the node is deleted from the solution domain and the iteration continued until a converged discrete solution is attained with the remaining N-1 nodes.

3.4 THE SOLUTION FEATURES

The adaptive numerical solution for the fluid speed, with varying numbers of nodes, in subsonic flow throughout the cone section is shown in FIG.5 and in supersonic flow in FIG.6; the final solution grid for each is indicated by a series of x's at the bottom of each figure.

The accuracy of the numerical solution of either flow type may be obtained by considering the relative difference between this solution and the exact solution of duct flow found in [1] by definition of an appropriate relative L_2 norm (see [2]). For the particular cone section flow considered here the exact solution for the fluid speed variation in subsonic flow is shown in FIG.4*i* and in supersonic flow in FIG.4*iii*, both taken from [1]. The relative error magnitudes corresponding to the numerical solutions shown in FIG.5 are presented in TABLE 1 and to those shown in FIG.6 in TABLE 2; these will be compared in accuracy to the respective solutions on a uniform fixed grid (see TABLE 3 from [2]). The number of iterations necessary for convergence of the fixed grid stage, 'IT - FG', and the number of sweeps required for the subsequent convergence of the adaptive grid stage, 'SW - AG', to within the specified convergence conditions (2.4) and (2.17) respectively, are also

given, together with the number of any node that has had to be deleted.

SUBSONIC CONVERGING CONE SECTION FLOW - ADAPTIVE GRID				
NODES	REL L2 ERROR	# IT - FG	# SW - AG	DELETE #
4	0.0000685	3	14	-
5	0.0000685	3	18	4
7	0.0000229	3	26	-
9	0.0000156	3	41	-
11	0.0000113	3	35	-

TABLE ONE

SUPERSONIC CONVERGING CONE SECTION FLOW - ADAPTIVE GRID				
NODES	REL L2 ERROR	# IT - FG	# SW - AG	DELETE #
5	0.0000214	3	12	-
6	0.0000117	3	18	-
8	0.00000719	3	25	-
9	0.00000719	3	21	6
10	0.00000488	3	65	-
11	0.00000488	3	71	8

TABLE TWO

CONVERGING CONE SECTION FLOW - FIXED GRID			
SUBSONIC FLOW		SUPERSONIC FLOW	
# NODES	RELATIVE L2 ERROR	# NODES	RELATIVE L2 ERROR
4	0.000116	5	0.0000279
7	0.0000283	6	0.0000177
9	0.0000158	8	0.00000891
11	0.0000101	10	0.00000535

TABLE THREE

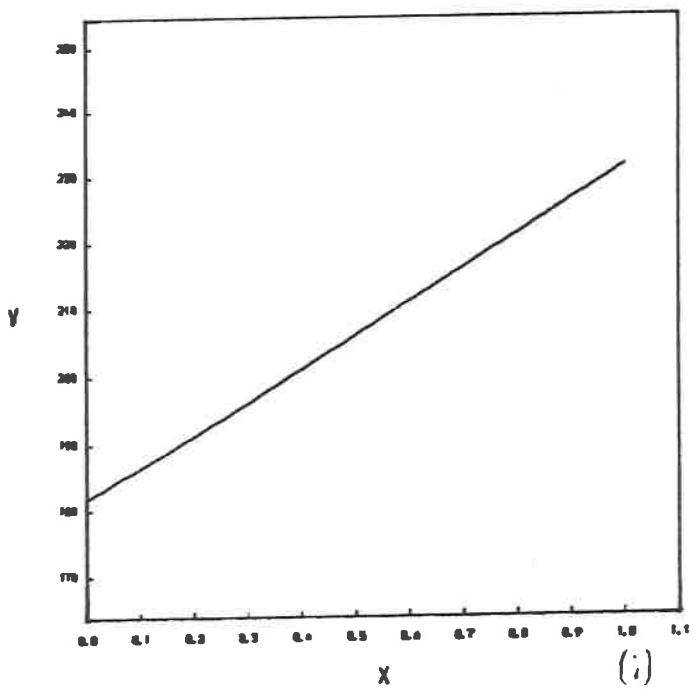

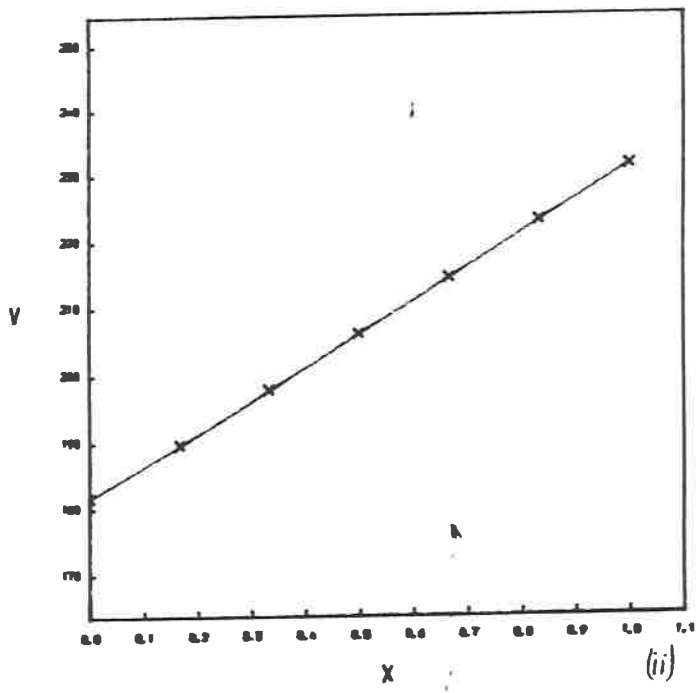

SUBSONIC FLOW

(i) EXACT PARAMETERIZATION

(ii) UNIFORM FIXED GRID SOLUTION

FIG. 4

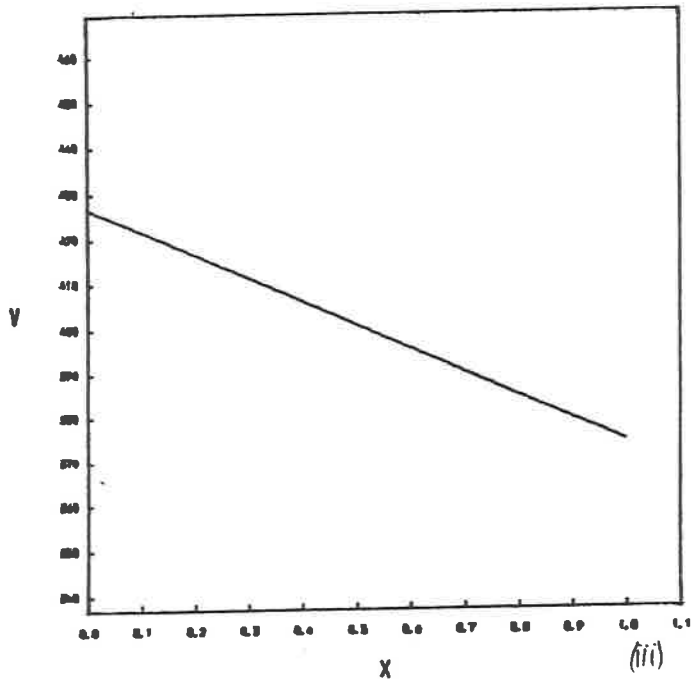

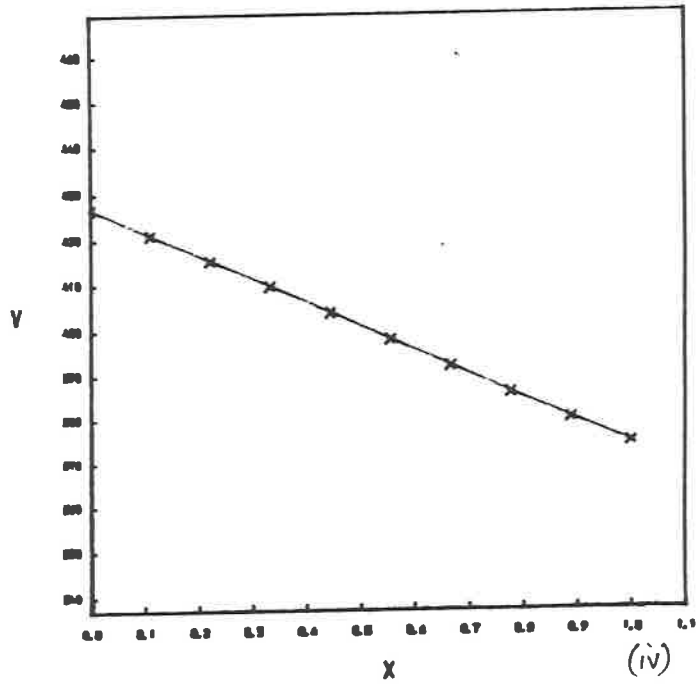

SUPERSONIC FLOW

(iii) EXACT PARAMETERIZATION

(iv) UNIFORM FIXED GRID SOLUTION

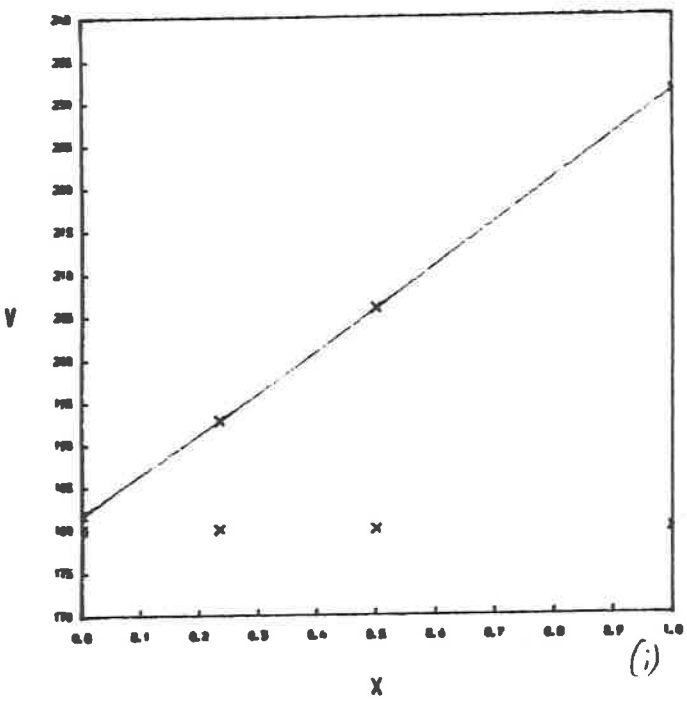

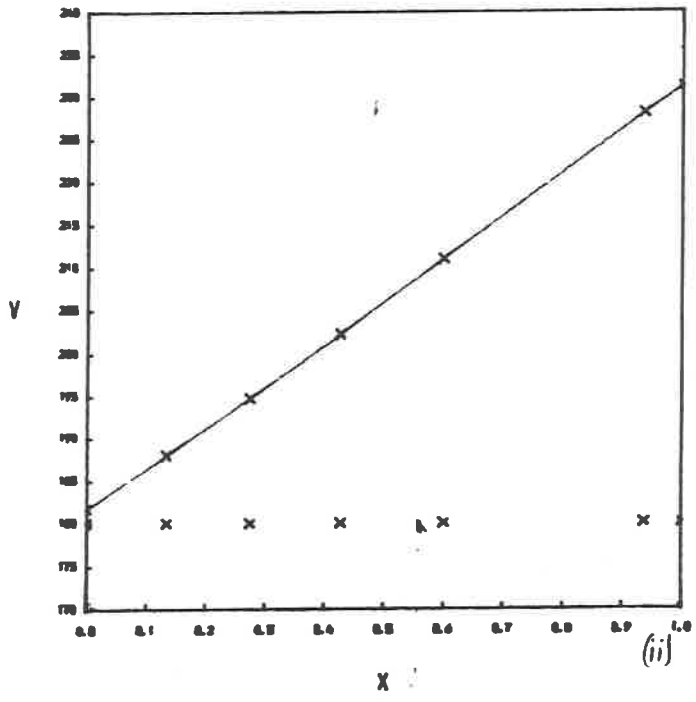

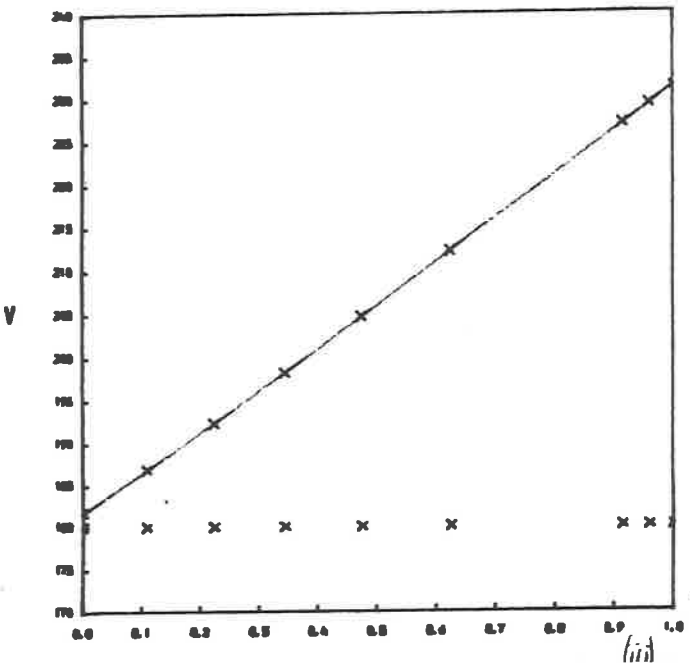

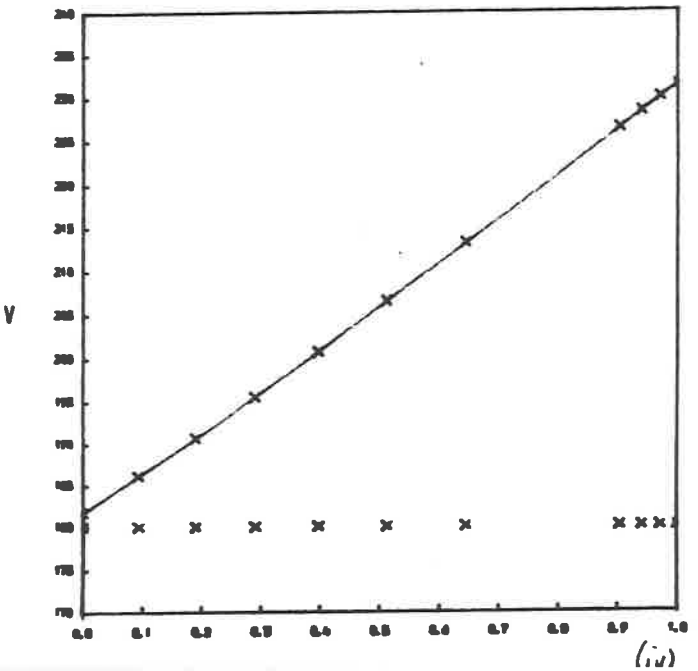

SUBSONIC FLOW
ADAPTIVE GRID SOLUTION
(i) 5 NODES
(ii) 7 NODES
(iii) 9 NODES
(iv) 11 NODES

FIG.5

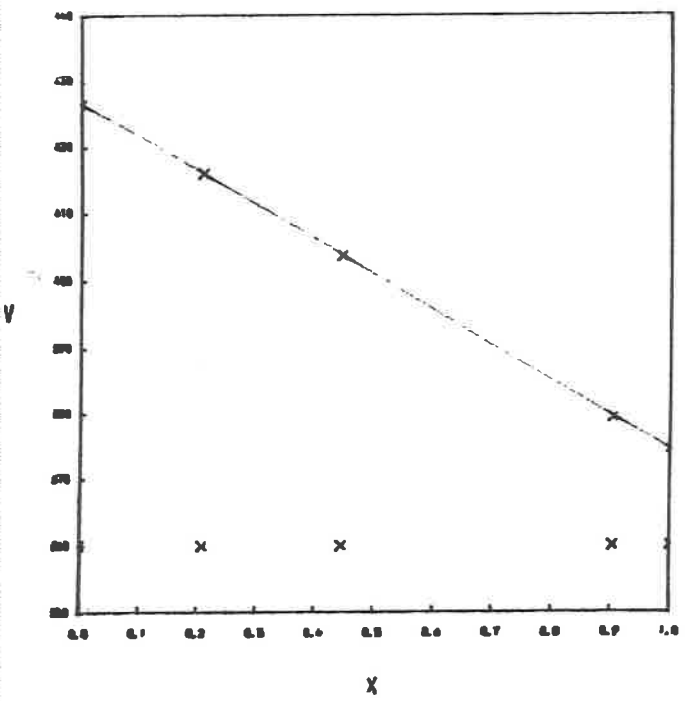

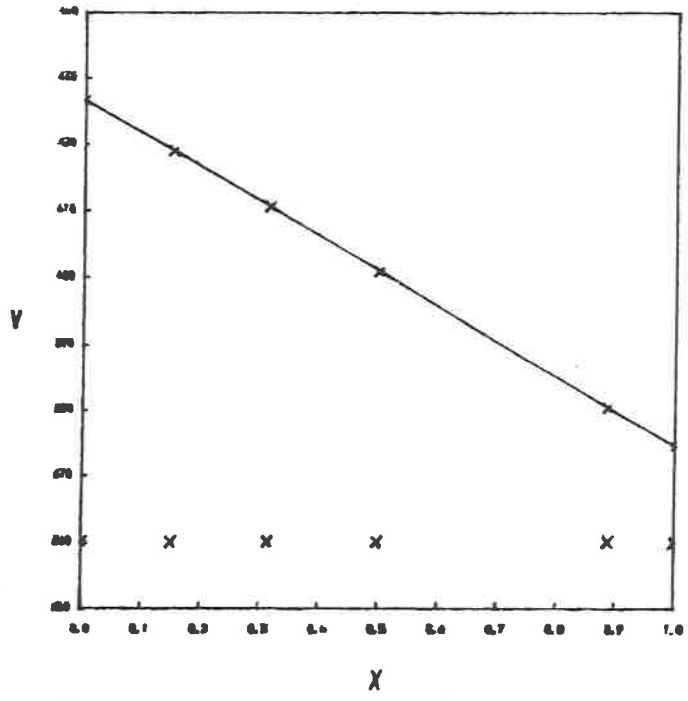

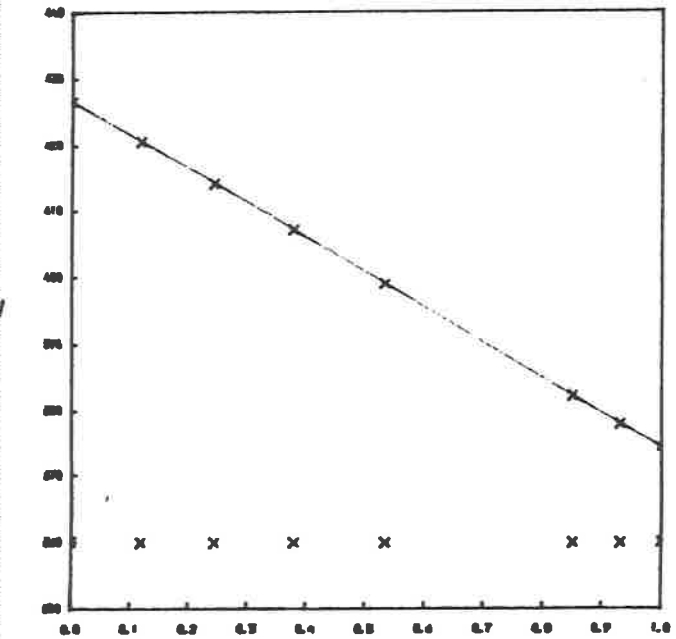

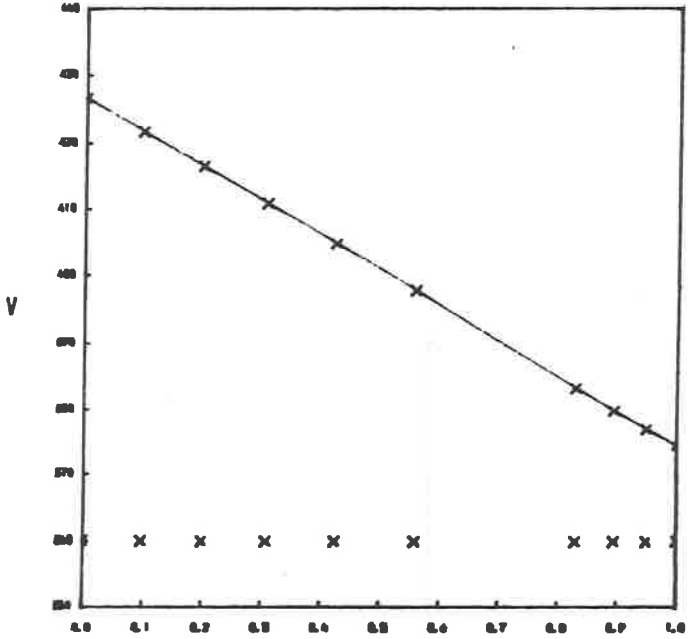

SUPERSONIC FLOW

ADAPTIVE GRID SOLUTION

(i) 5 NODES

(ii) 6 NODES

(iii) 9 NODES

(iv) 10 NODES

FIG.6

Subsonic flow

On employing five nodes in the numerical solution of subsonic flow on employing five nodes it is found that, owing to the singularity of $[J]_i^k$, node 4 must be deleted (see §3.3) and thus the final solution vector has four nodes (see FIG.5*i*). In fact exactly the same final solution vector is obtained on employing four nodes initially in the discrete solution, which is consistent with the corresponding relative error magnitudes shown in TABLE 1. The solution can, from TABLE 3, be seen to be more accurate, in terms of the L_2 norm, than that obtained by employing four nodes on a uniforn fixed grid. The improved accuracy is again seen on using seven nodes in the solution, note the linear region in the solution clearly seen in FIG.5*ii*.

When employing even more nodes in the discrete solution, although node merging does not result, considerable migration of nodes is caused by the presence of the linearity (see FIGS.5*iii*,*iv*). Thus nodes can be seen to 'bunch' towards the right hand side of the solution domain impairing the relative accuracy of the solution. In fact for nine nodes the adaptive grid solution is only marginally better, in terms of the error norm, than the fixed grid equivalent and for eleven nodes actually becomes less accurate. The representation of the solution features on an adaptive grid though are vastly improved; the detection of the linear region in the fixed grid solution (FIG.4*ii*) is impossible, but may of course be verified retrospectively by close inspection of the associated exact solution (FIG.4*i*).

Supersonic flow

The numerical solution, using either five or six nodes (FIGS.6*i*.*ii*), in the approximation of the fluid speed in supersonic flow may be seen, comparing TABLES 2 and 3, to be more accurate than when solving on a fixed uniform grid. On solving with nine nodes in the solution (see FIG.6*iii*) a node must be deleted (see TABLE 2); again on solving initially with one less node, i.e. eight nodes, the same converged solution vector is obtained. The relative accuracy of this formulation, and that using ten nodes (see FIG.6.*iv*), although an improvement on the fixed grid equivalent is again impaired due to the migration of the nodes as a consequence of a linear region in the exact solution.

3.5 THE NODAL TRAJECTORIES

The features of the numerical solutions of §3.4, in particular the occurrence of node deletion, are clearly illustrated by inspection of the nodal displacements and nodal amplitudes of the current solution vector at each iteration level on the adaptive grid. The trajectories of the nodes, in both cases, throughout convergence to the approximation to the steady state solution may then be obtained.

The trajectories associated with the numerical solution of the fluid speed in subsonic cone section flow employing initially five and eleven nodes are shown; note the uniform starting displacement of the nodes in each case, i.e. at the converged solution stage on the fixed grid (see FIGS.7*i*,8*i*). The generally smooth trajectories associated with solution on the adaptive grid then proceed until convergence is reached

after the required number of iterations (TABLE 1). A particular feature of FIGS.7*i*,*ii* is the near merging of nodes 3 and 4 after just two iterations on the adaptive grid, followed by the deletion of node 4 at the specified tolerance: the solution can then be seen to correct significantly as iteration now proceeds with one less node. In FIGS.8*i*,*ii* note the immediate rapid migration of nodes 8, 9 and 10 due to the linearity present, bunching towards the right hand side of the solution domain, and their subsequent representation of the curvature in this region.

The nodal trajectories provided for the numerical solution of the fluid speed in supersonic cone section flow have been chosen so as to illustrate the effect on the final solution vector of deleting a node from the solution domain. The nodal trajectories, in displacement and amplitude, when initially solving with nine nodes (see FIG.9) clearly show the deletion of node 6 and more importantly the subsequent convergence to the same solution vector obtained when only eight nodes are used (see FIG.10).

3.6 FLOW PARAMETERISATION

The remaining flow variables associated with a cone section motion may be related to the fluid speed by a set of algebraic relationships (see [1] or [5]). By considering a piece-wise linear approximation to the fluid speed as a parameterisation of the flow, substitution of this into the relationships allows the derivation of the piece-wise linear variation of all the other flow variables in the motion; this is shown for subsonic flow, solving with seven adaptive nodes, in FIG.11 and for supersonic flow, when using ten nodes, in FIG.12.

SUBSONIC FLOW
NODAL TRAJECTORIES
FIVE NODES

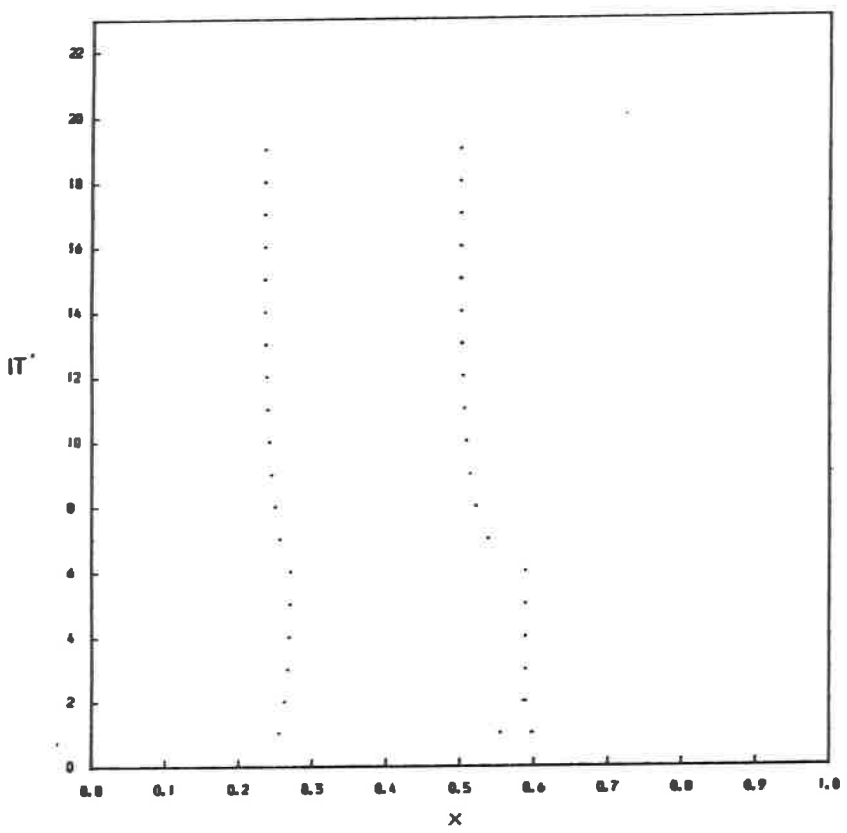

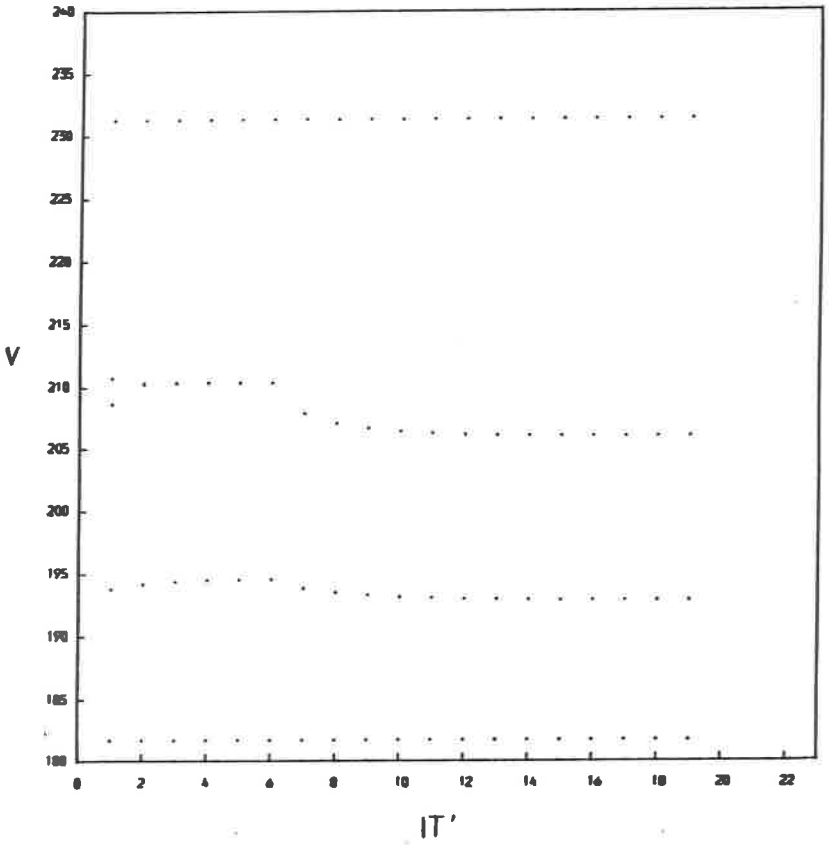

FIG. 7

SUBSONIC FLOW
NODAL TRAJECTORIES
ELEVEN NODES

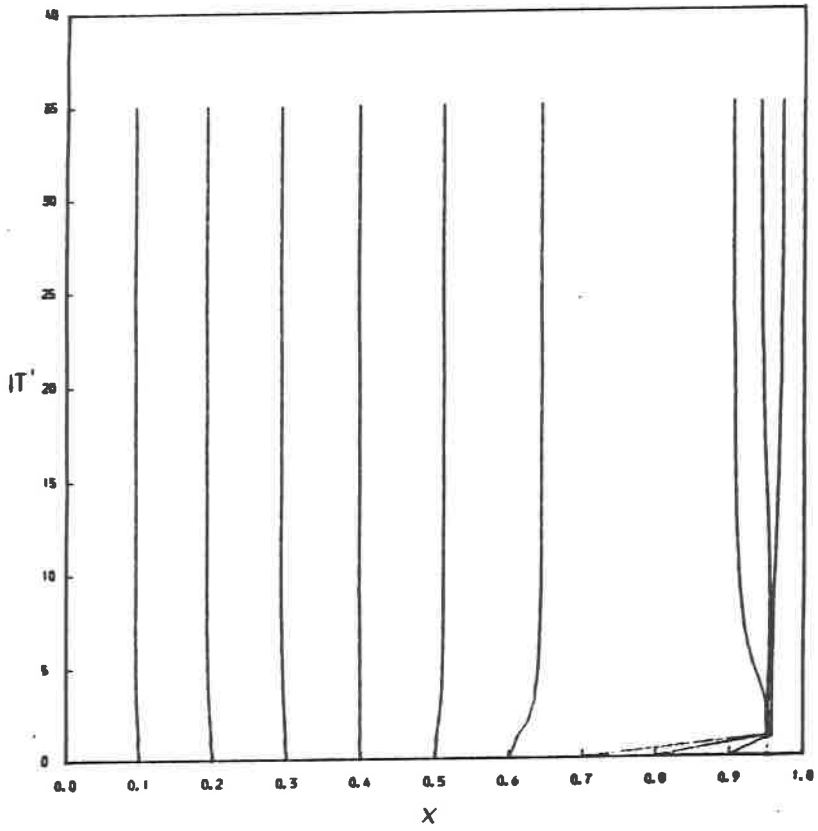

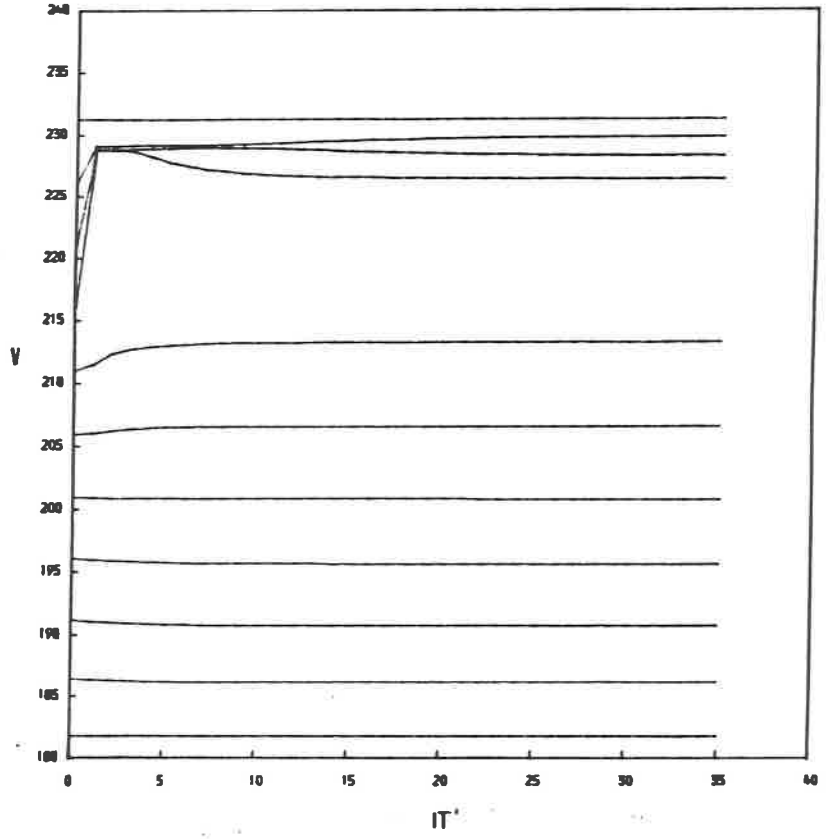

FIG. 8

SUPERSONIC FLOW
NODAL TRAJECTORIES
NINE NODES

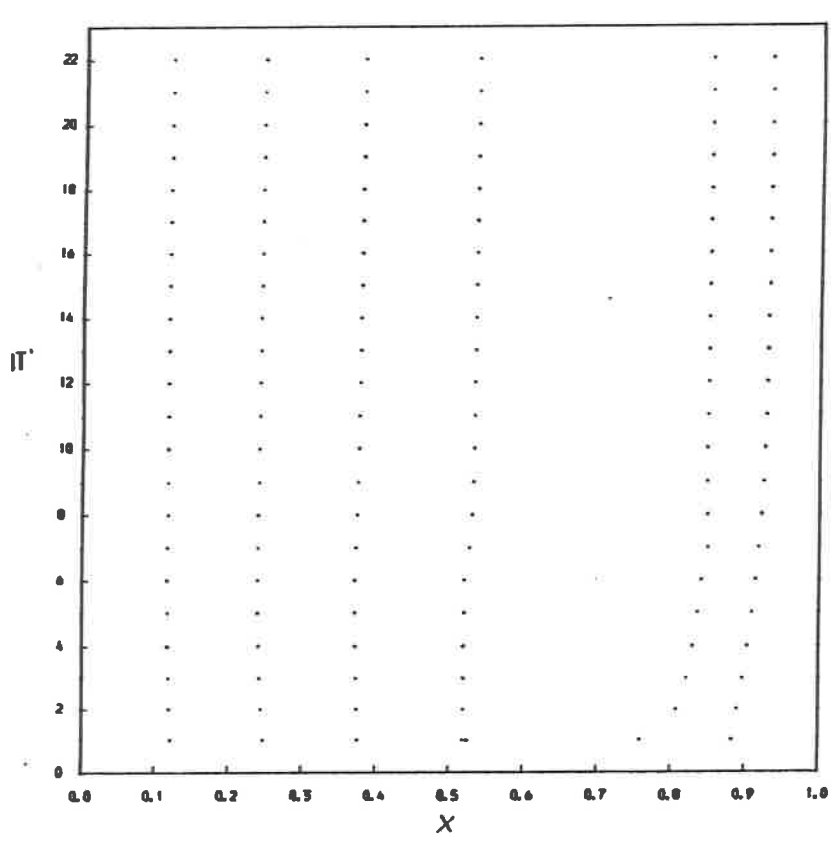

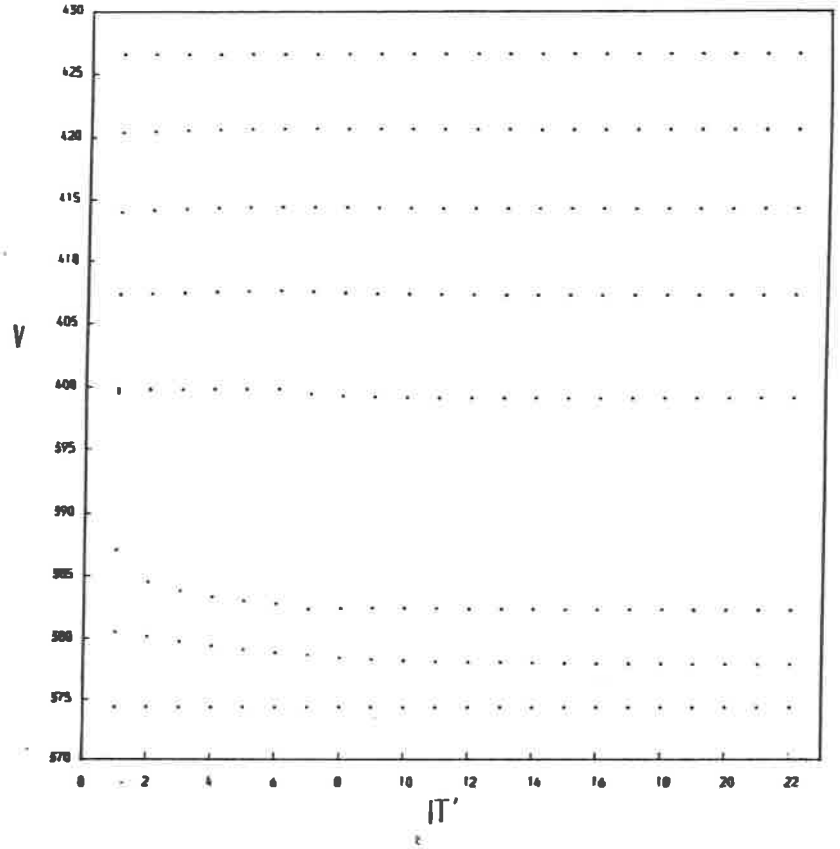

FIG. 9

SUPERSONIC FLOW
NODAL TRAJECTORIES
EIGHT NODES

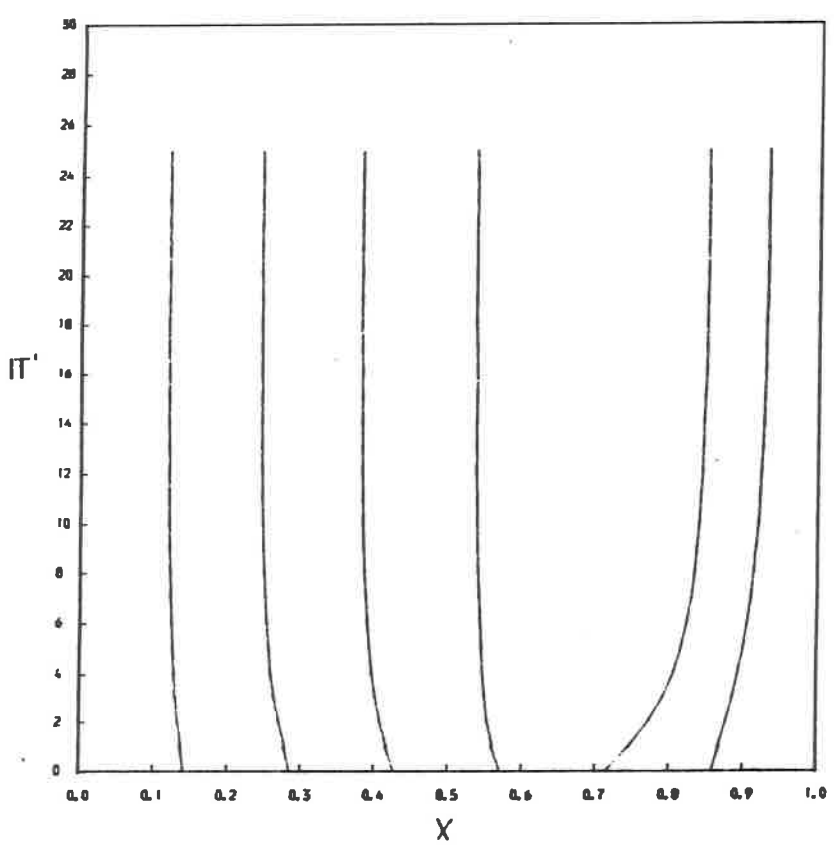

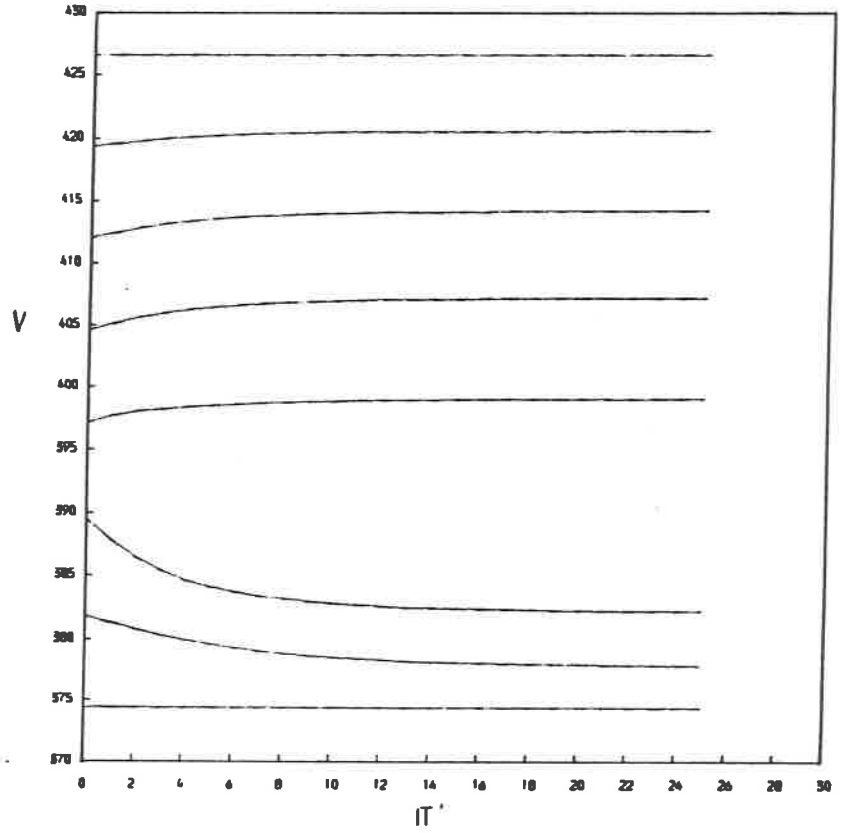

FIG. 10

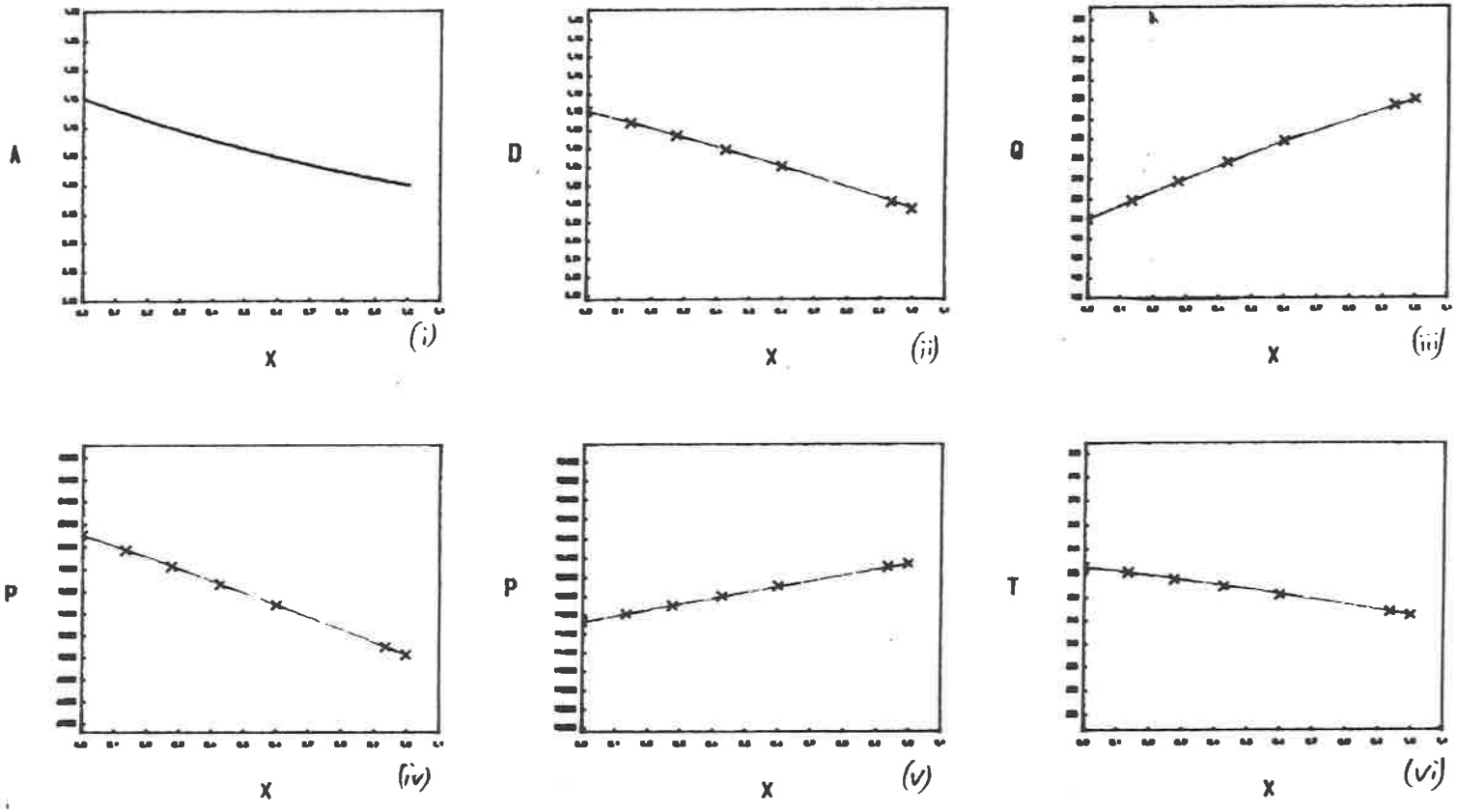

SUBSONIC FLOW
FLOW VARIABLE VARIATION
7 NODES

FIG. 11

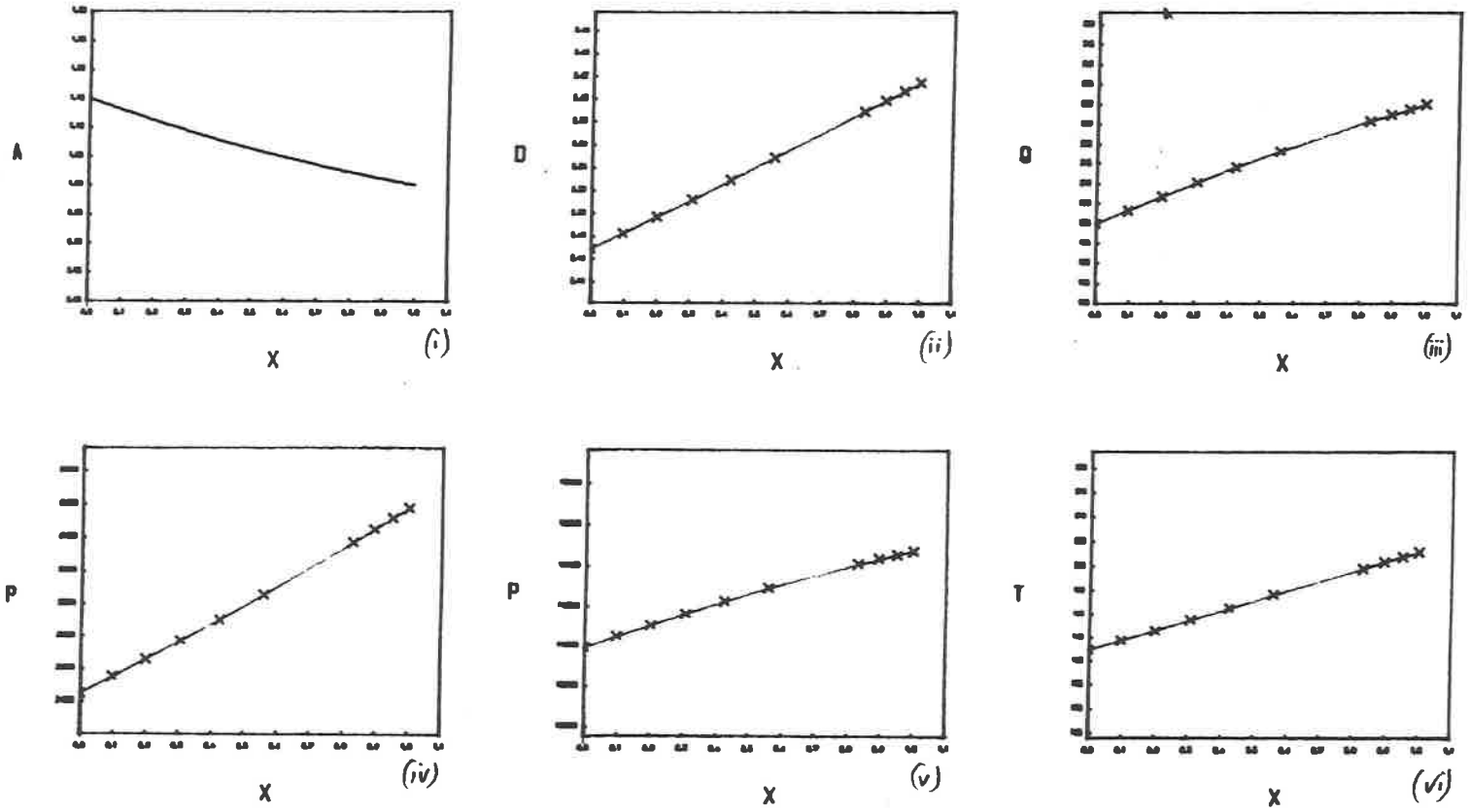

SUPERSONIC FLOW
FLOW VARIABLE VARIATION
TEN NODES

FIG. 12

SECTION FOUR : THE ADAPTIVE GRID SOLUTION OF DE-LAVAL NOZZLE FLOW

The adaptive grid method is now applied to the approximate solution of flow through a de-Laval nozzle. The results obtained are compared with the approximate solution of the same motion on both a uniform and irregular fixed grid (see [2]).

4.1 DEFINITION OF MOTION

The de-Laval nozzle is defined on the domain

$$0.0 \leq x \leq 2.0 \ , \tag{4.1}$$

by the area variation corresponding to the two composite sections

$$\begin{aligned} &\text{ENTRY SECTION} \quad : A_1(x) = 1.1 - (x/8) && 0.0 \leq x \leq 0.8 \ , \\ &\text{EXHAUST SECTION} \quad : A_2(x) = (2.6/3.0) + (x/6) && 0.8 \leq x \leq 2.0 \ , \end{aligned} \tag{4.2}$$

with

$$\begin{aligned} A_e &= 1.1 \ , \\ A_T &= 1.0 \\ \text{and} \quad A_o &= 1.2 \ . \end{aligned} \tag{4.3}$$

where A_T is the minimum cross-sectional area of the nozzle at the throat location, i.e. from (4.2) at $x = 0.8$. The mass flow inlet condition is assigned by setting

$$C = 223.9193 \ , \tag{4.4}$$

so that the mass flow rate value at the throat, Q_T, is the critical value, Q_*, where

$$Q_T = Q_* = 246.31124 \ , \tag{4.5}$$

and the outlet mass flow boundary condition then becomes

$$Q_o = 205.25936 \ , \tag{4.6}$$

(see [2]). The stationary principle corresponding to this motion, by substitution of (4.3a) and (4.4) into (1.11), is

$$\delta \left[\int_D \left[\frac{246.31124}{A(x)} v + p(v) \right] dx \right] = 0 \ , \tag{4.7}$$

where $A(x)$ is defined by (4.2).

4.2 THE IMPLEMENTATION OF THE SYSTEM SOLUTION ALGORITHM

The approximate fluid speed variation throughout the nozzle is again obtained in two stages. The problem is solved initially on a fixed grid, where the domain length is

$$d = 2.0 \ , \tag{4.8}$$

defined by (2.2) and (2.3) such that a node always lies at the nozzle throat.

The flow is assumed to enter the nozzle subsonically: the flow being critical at the throat (4.5) means that, dependent on the outlet pressure conditions, it may remain so throughout the complete nozzle or a transition may occur at the nozzle throat to supersonic flow (see [1]).

The approximate fluid speed solution on the fixed grid in subsonic flow, $\underline{a}^*_{Fsub}$, is obtained by specifying the constant initial data vector (3.5a) (see FIG.13*ii* when employing twenty-one nodes). The approximation to transition flow, $\underline{a}^*_{Ftrans}$, is found by first computing the supersonic flow solution, by specifying (3.5b), and then taking a linear combination (see [2]) of these two solution vectors about the throat node (see FIG.13*iv* when using twenty-one nodes). The computed amplitude of the throat node, $\underline{a}^*_T$, in the converged fixed grid solution of both flow types may be, again because the flow is critical at the throat, overwritten by the exact sonic value, i.e.

$$\underline{a}^*_T = 302.5 \ , \tag{4.9}$$

but whether this is actually carried out depends on the particular treatment of the throat node in the adaptive grid stage.

4.3 THE NOZZLE SOLUTION - CONSTRAINED THROAT NODE

The basic solution algorithm (§2) is modified for the present approximate solution of nozzle flow such that a node is constrained to remain positioned at the nozzle throat, although it may still vary in amplitude. The throat node amplitude in the fixed grid solution of transition flow is not overwritten by the exact solution (4.9) as initial data in this case because the resulting linearity (see FIGS.13*iv*) causes nodes to merge in the adaptive grid stage of the solution. Numerically the throat node constraint may be implemented by overwriting the associated local system (2.11) at each iteration level by

$$\begin{bmatrix} A & 0 \\ 0 & 1 \end{bmatrix} \begin{bmatrix} \delta a_T^k \\ \delta s_T^k \end{bmatrix} = - \begin{bmatrix} F_{TL}^k \\ 0 \end{bmatrix} , \qquad (4.10)$$

where the subscript T refers to the throat node and A is defined corresponding to (2.12). Then by inspection of (4.10) the updates to the throat node are

$$\delta s_T^k = 0.0$$

and (4.11)

$$\delta a_T^k = - \frac{F_{TL}^k}{A} .$$

The approximation to the fluid speed in subsonic flow, when using twenty-one nodes on the adaptive grid, is shown in FIG.14 and the approximation to transition flow in FIG.14. The final solution grids are again indicated on these figures by a series of x's and are also available explicitly from TABLE 4. Note that, as would be expected, the

computed grid is the same in the entry section for the numerical solution of both flow types.

NUMERICAL SOLUTION GRID FOR TWENTY-ONE NODES						
	ADAP' GRID CONS		ADAP' GRID FIX		FIX' GRID - IRR	
NODE #	SUB'	TRANS'	SUB'	TRANS'	SUB'	TRANS'
1	0.0000	0.0000	0.0000	0.0000	0.0000	0.0000
2	0.1777	0.1777	0.1909	0.1909	0.1820	0.1820
3	0.3335	0.3335	0.3563	0.3563	0.3540	0.3540
4	0.4673	0.4673	0.4961	0.4961	0.4960	0.4960
5	0.5790	0.5790	0.6100	0.6100	0.6140	0.6140
6	0.6683	0.6683	0.6978	0.6978	0.6900	0.6900
7	0.7351	0.7351	0.7591	0.7591	0.7370	0.7370
8	0.7790	0.7790	0.7938	0.7938	0.7720	0.7720
9	0.8000	0.8000	0.8000	0.8000	0.8000	0.8000
10	0.8153	0.8017	0.8041	0.8048	0.8200	0.8210
11	0.8466	0.8219	0.8274	0.8286	0.8450	0.8450
12	0.8939	0.8605	0.8686	0.8700	0.8760	0.8770
13	0.9569	0.9173	0.9273	0.9288	0.9190	0.9200
14	1.0353	0.9920	1.0033	1.0047	0.9850	0.9860
15	1.1289	1.0843	1.0963	1.0974	1.0740	1.0750
16	1.2374	1.1940	1.2060	1.2068	1.1800	1.1810
17	1.3606	1.3209	1.3320	1.3325	1.3080	1.3080
18	1.4984	1.4648	1.4744	1.4747	1.4570	1.4560
19	1.6508	1.6258	1.6331	1.6331	1.6290	1.6270
20	1.8180	1.8041	1.8082	1.8082	1.8220	1.8200
21	2.0000	2.0000	2.0000	2.0000	2.0000	2.0000

ADAP' GRID CONS : ADAPTIVE GRID SOLUTION - CONSTRAINED THROAT NODE.

ADAP' GRID FIX : ADAPTIVE GRID SOLUTION - FIXED THROAT NODE.

FIX' GRID IRR : FIXED IRREGULAR GRID SOLUTION.

TABLE FOUR

The magnitude of the relative errors, in comparison to the exact solutions from [1] (see FIGS.13*i*,*iii*), for the approximate solution of both flow types with varying numbers of nodes are found in TABLE 5. Note the increase in relative accuracy in all cases over the equivalent

solution on a fixed uniform grid, and additionally over that on a fixed irregular grid, computed (see [2]) by polynomial interpolation of the exact solution and equi-distribution of the nodes (see TABLE 6). The number of sweeps necessary for convergence in the fixed grid stage for every formulation considered is three and the number required on the adaptive grid, 'SW' is shown in the table; note that no nodes have been deleted from the solution domain.

ADAPTIVE GRID SOLUTION OF DE-LAVAL NOZZLE FLOW - THROAT CON					
SUBSONIC FLOW			TRANSITION FLOW		
NODE #	REL L2 ERR	# SW'	NODE #	REL L2 ERR	# SW'
11	0.002369	59	11	0.001663	59
15	0.001398	117	15	0.001012	118
21	0.001011	188	21	0.000766	189

TABLE FIVE

FIXED GRID SOLUTION OF DE-LAVAL NOZZLE FLOW - REL L2 ERROR					
SUBSONIC FLOW			TRANSITION FLOW		
NODE #	UNIFORM	IRREGULAR	NODE #	UNIFORM	IRREGULAR
11	0.0158	0.0041	11	0.0095	0.0028
15	0.0105	-	15	0.0063	-
21	0.0078	0.0014	21	0.0047	0.0010

TABLE SIX

ADAPTIVE GRID SOLUTION OF DE-LAVAL NOZZLE FLOW - THROAT FIX					
SUBSONIC FLOW			TRANSITION FLOW		
NODE #	REL L2 ERR	# SW'	NODE #	REL L2 ERR	# SW'
11	0.001875	60	11	0.001298	60
15	0.000906	119	15	0.000634	119
21	0.000868	191	21	0.000633	191

TABLE SEVEN

4.4 THE NOZZLE SOLUTION - FIXED THROAT NODE

The basic solution algorithm is now adapted by fixing the throat node, not only at the throat location, but additionally in amplitude at the exact sonic speed given in (4.9). This now becomes an internal numerical boundary condition and numerically the updates to the amplitude and displacement of the throat node at each iteration level are overwritten by zero. The fixed grid solution vectors for each flow type, illustrated in FIGS.13*ii*,*iv*, may now be used as the initial data for the adaptive grid stage.

The adaptive grid solution for the fluid speed in both flow types, using twenty-one nodes, are shown in FIGS.16,17 with, as previously, the final solution grid denoted by 'x'. On comparison with the approximate solutions in FIGS.14,15 it may be seen that there is an improvement, over when the throat node was constrained in position only, in the representation of the curvature in the solution around the nozzle throat; this is probably due to the inaccuracy of the numerical quadrature and thus of the throat node amplitude in representing the extreme gradients at the throat. The relative error magnitudes for

various numerical solutions of both flow types, using the present treatment of the throat node, are provided in TABLE 7, and these can be seen to be more accurate than those on both of the fixed grids (see TABLE 6) and also as expected the previous adaptive grid solution §4.3 (see TABLE 5).The improved nodal distribution can also be seen on inspection of the exact final nodal positions provided in TABLE 4; again note that the numerical grids are the same throughout the entry section.

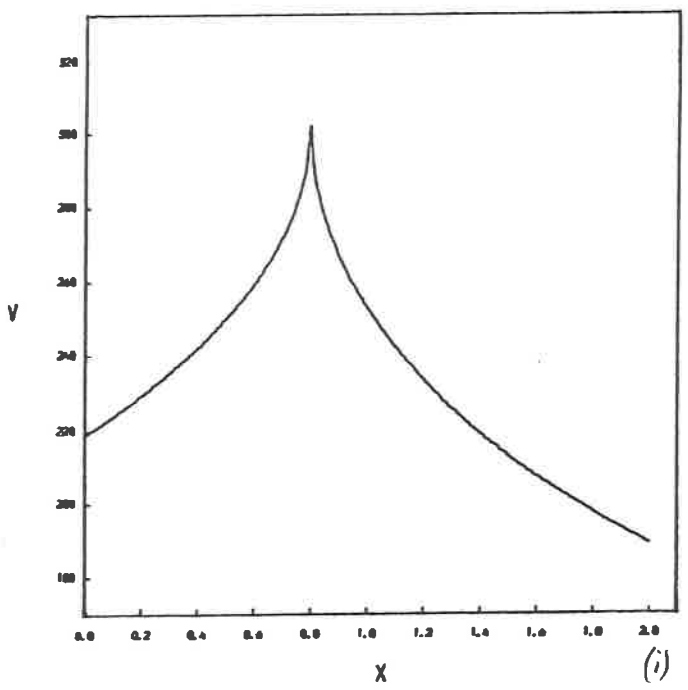

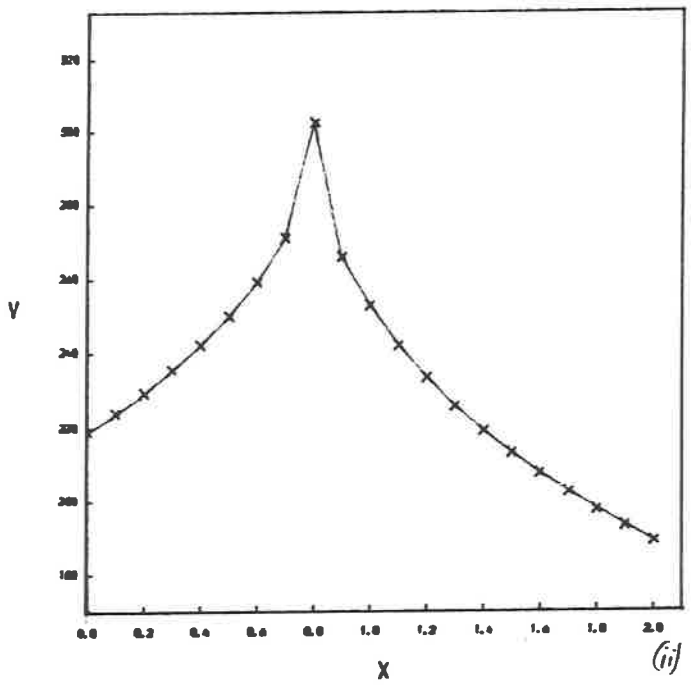

SUBSONIC FLOW

(i) EXACT PARAMETERIZATION

(ii) UNIFORM FIXED GRID SOLUTION

FIG. 13

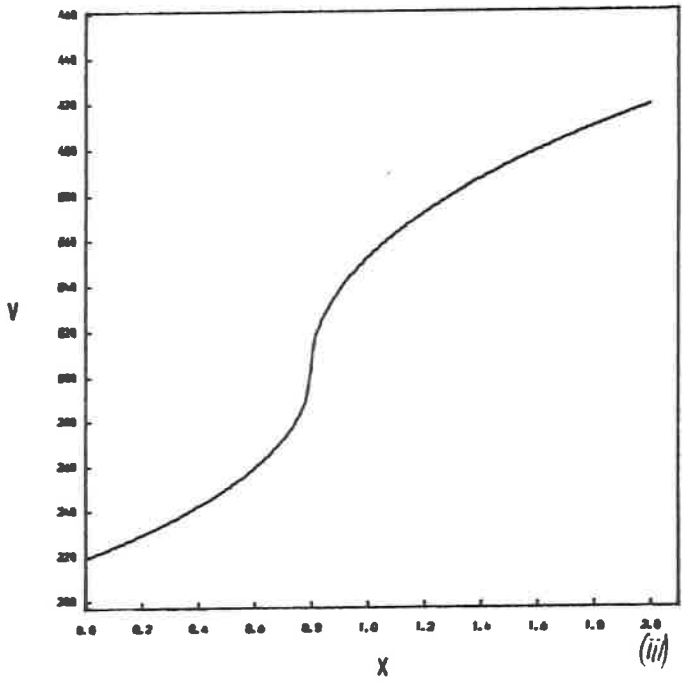

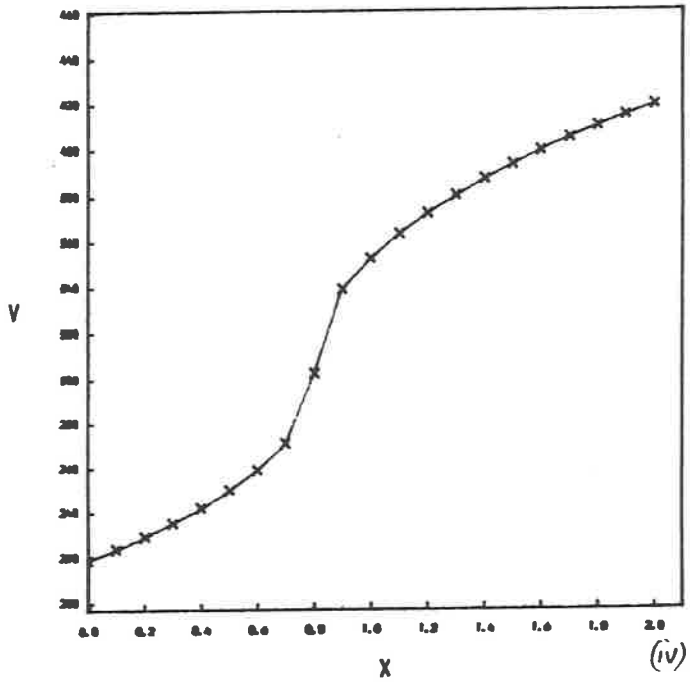

TRANSITION FLOW

(iii) EXACT PARAMETERIZATION

(iv) UNIFORM FIXED GRID SOLUTION

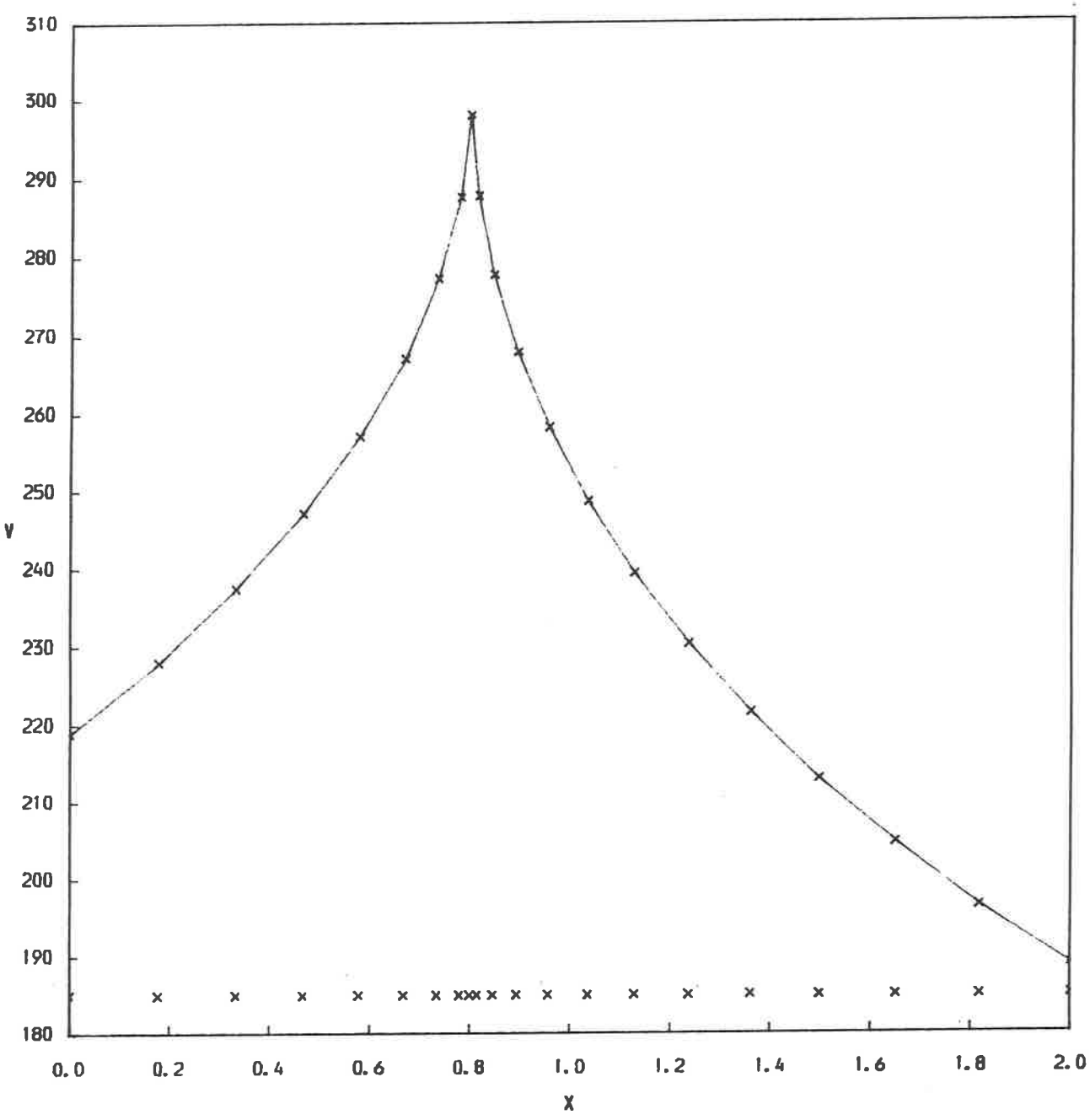

SUBSONIC FLOW
ADAPTIVE GRID SOLUTION
CONSTRAINED THROAT NODE
21 NODES

FIG. 14

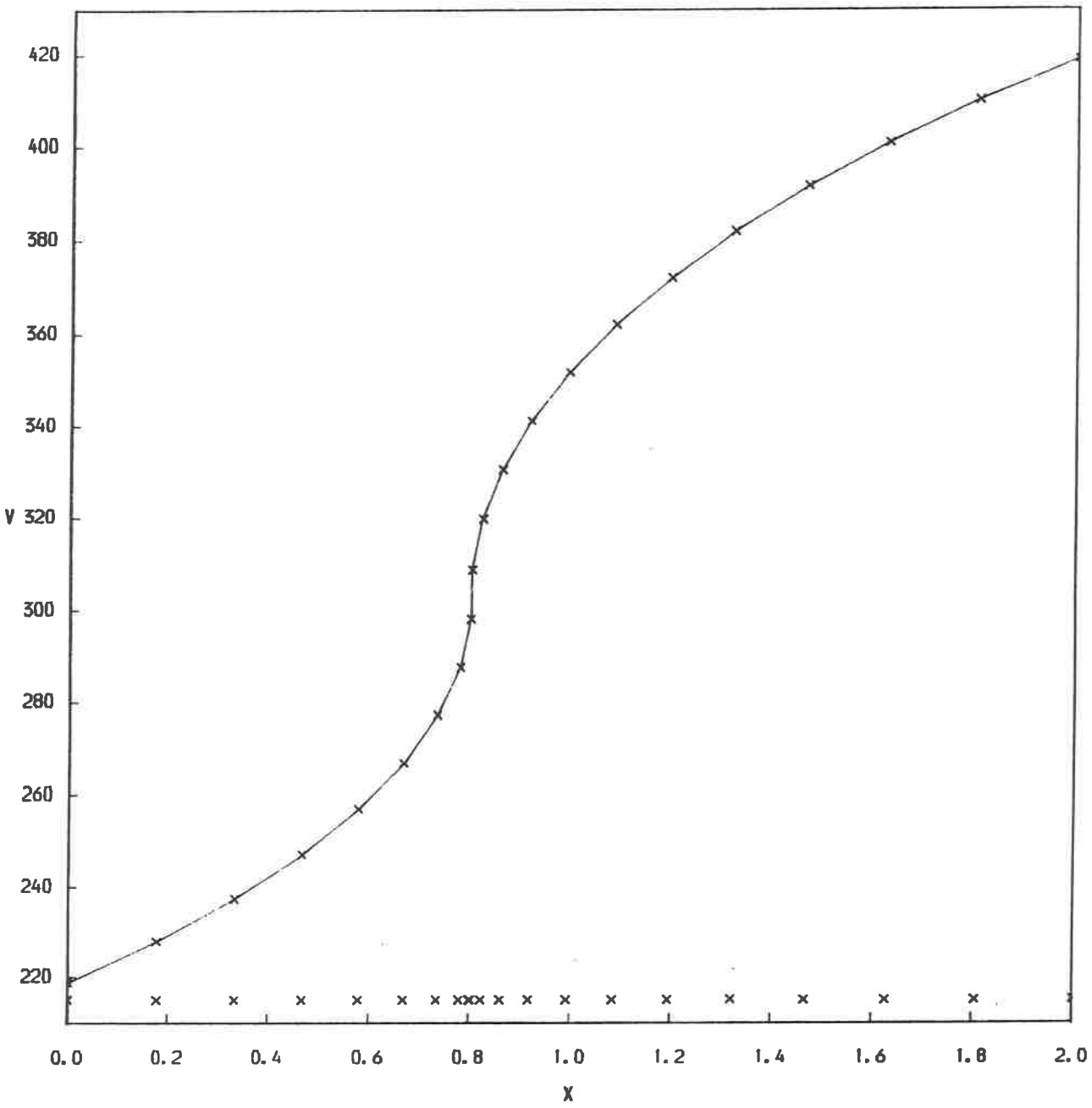

TRANSITION FLOW
ADAPTIVE GRID SOLUTION
CONSTRAINED THROAT NODE
21 NODES

FIG. 15

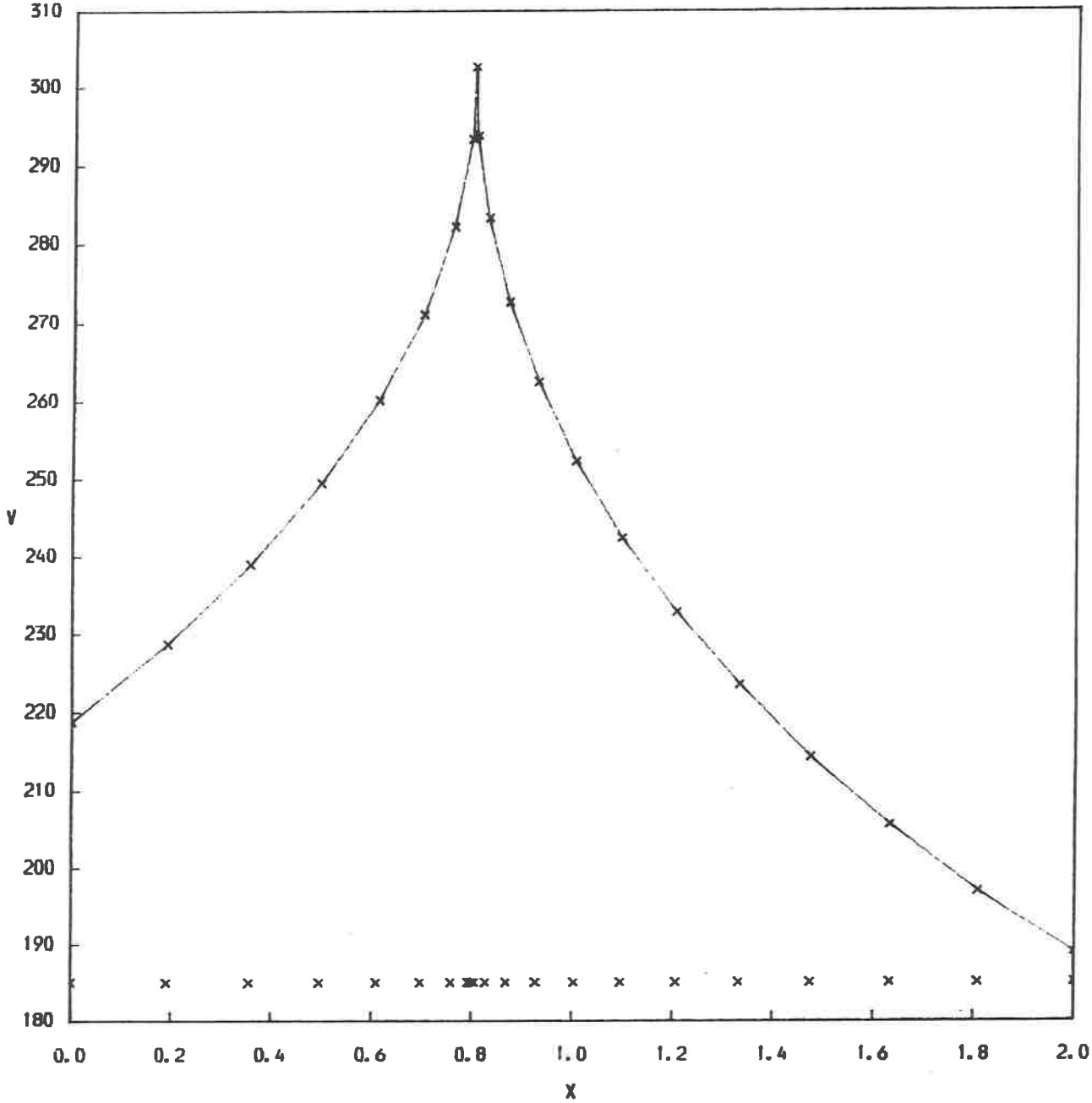

SUBSONIC FLOW
ADAPTIVE GRID SOLUTION
FIXED THROAT NODE
21 NODES

FIG. 16

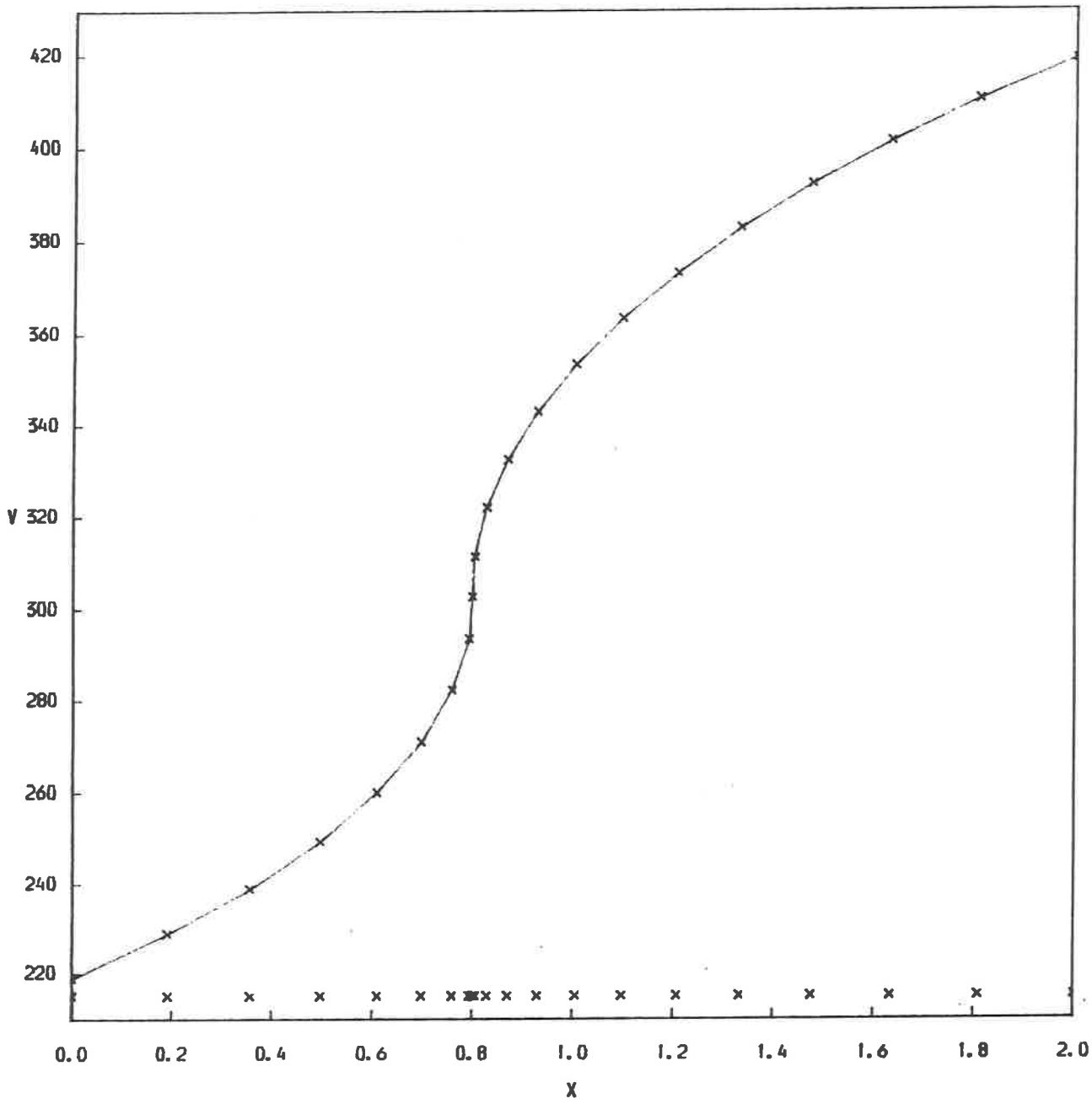

TRANSITION FLOW
ADAPTIVE GRID SOLUTION
FIXED THROAT NODE
21 NODES

FIG.17

4.5 THE UPDATE OF THE LOCAL SYSTEM

The possibility of modifying the basic algorithm such that each node is locally updated more than once has been suggested in §2.1. The effect on the solution, with particular regard to the number of sweeps required for convergence on the adaptive grid and the consequent final solution vector, has been studied when considering each of the treatments, §4.3 and §4.4, of updating the throat node. The results are shown in TABLES 8 and 9.

ADAPTIVE GRID SOLUTION - THROAT CONS' - LOCAL ITERATIONS					
SUBSONIC FLOW			TRANSITION FLOW		
LOC' IT'	REL L2 ERR	# SW'	LOC' IT'	REL L2 ERR	# SW'
1	0.00101	188	1	0.000766	189
2	0.00101	181	2	0.000766	182
3	0.00101	181	3	0.000766	182

TABLE EIGHT

ADAPTIVE GRID SOLUTION - THROAT FIX'D - LOCAL ITERATIONS					
SUBSONIC FLOW			TRANSITION FLOW		
LOC' IT'	REL L2 ERR	# SW'	LOC' IT'	REL L2 ERR	# SW'
1	0.000868	191	1	0.000633	191
2	0.000868	184	2	0.000633	184
3	0.000868	184	3	0.000633	183

TABLE NINE

First note that the final approximate solution vector for each motion studied, when employing the same throat node treatment, is the same however many local iterations, 'LOC IT', are performed; this is reflected in the relative error values. It may also be seen that in the solution of every motion there is a decrease in the number of sweeps required for convergence on the adaptive grid when each of the nodes are updated twice in turn. A further increase in the number of local iterations has no effect on the necessary number of sweeps, from which it may be concluded that after two iterations the local system (2.11) for each node has to all intents and purposes converged. The node is then optimally placed with respect to its neighbours. It must be noticed however that in real terms twice as many computations are now carried out per sweep and thus in terms of expense the inclusion of this as a feature of the solution algorithm is not worthwhile.

4.6 THE NODAL TRAJECTORIES

The trajectories of the nodes with respect to displacement and amplitude, when using twenty-one nodes and constraint of the throat node (§4.3), for the approximation to the fluid speed in subsonic flow are shown in FIG.18 and in transition flow in FIG.19. Note the initial uniform displacement of the nodes in FIGS.18*i*,19*i* at the converged solution on the fixed grid, and also that the broken lines in FIG.18*ii* represent the nodal amplitude trajectories in the nozzle diffuser. Similarly the trajectories of the nodes in the approximate solution of both flow types with the throat node fixed are found in FIGS.20,21; the additional feature of these graphs is the constant throat node amplitude shown in FIGS.20*ii*,21*ii*.

4.7 FLOW PARAMETERIZATION

The piece-wise linear variation of the remaining flow variables associated with a nozzle motion may again be obtained by considering a piecewise linear fluid speed variation to give a particular parameterization of the flow. The variation of each of these variables for both subsonic and transition flow, when employing twenty-one nodes and fixing the throat node are shown in FIGS.22,23 respectively.

SUBSONIC FLOW
NODAL TRAJECTORIES
CONSTRAINED THROAT NODE
21 NODES

FIG. 18

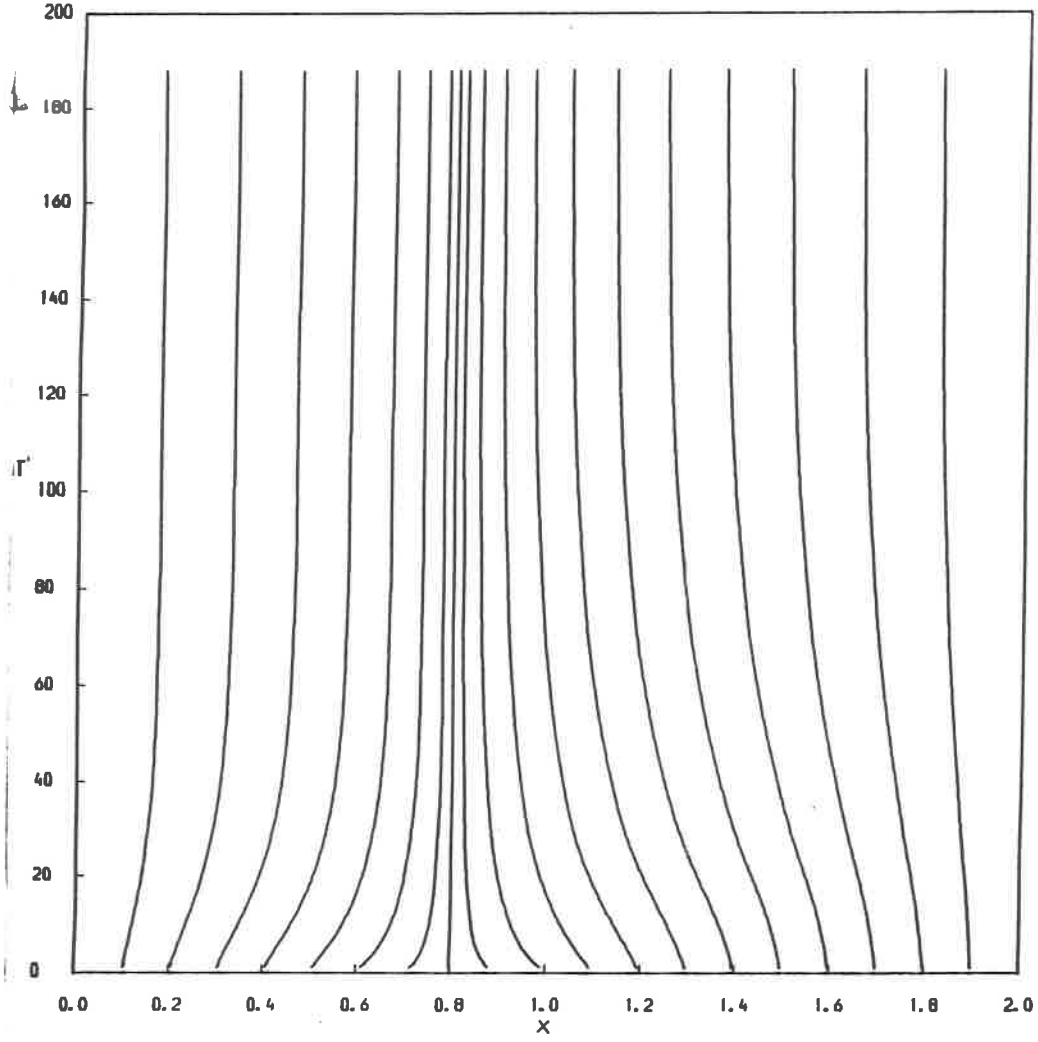

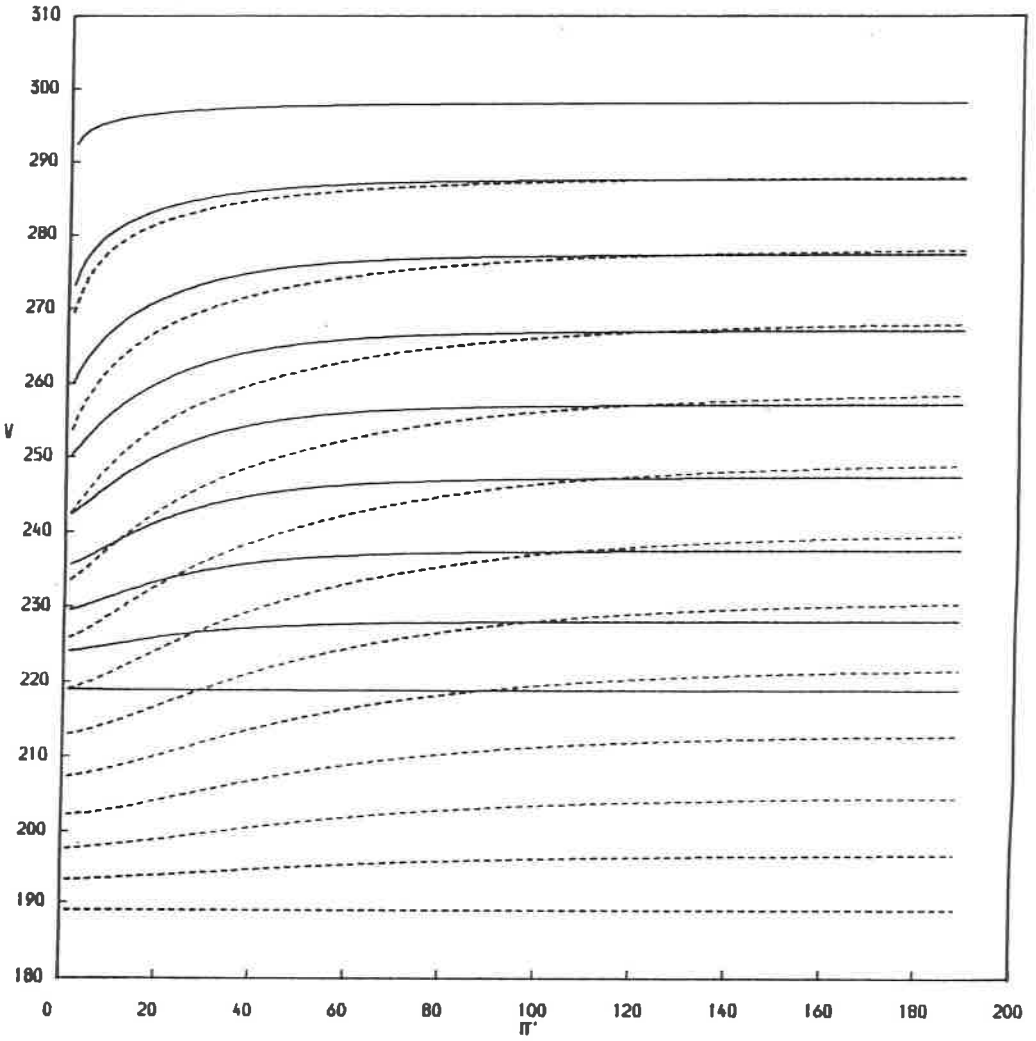

TRANSITION FLOW
NODAL TRAJECTORIES
CONSTRAINED THROAT NODE
21 NODES

FIG.19

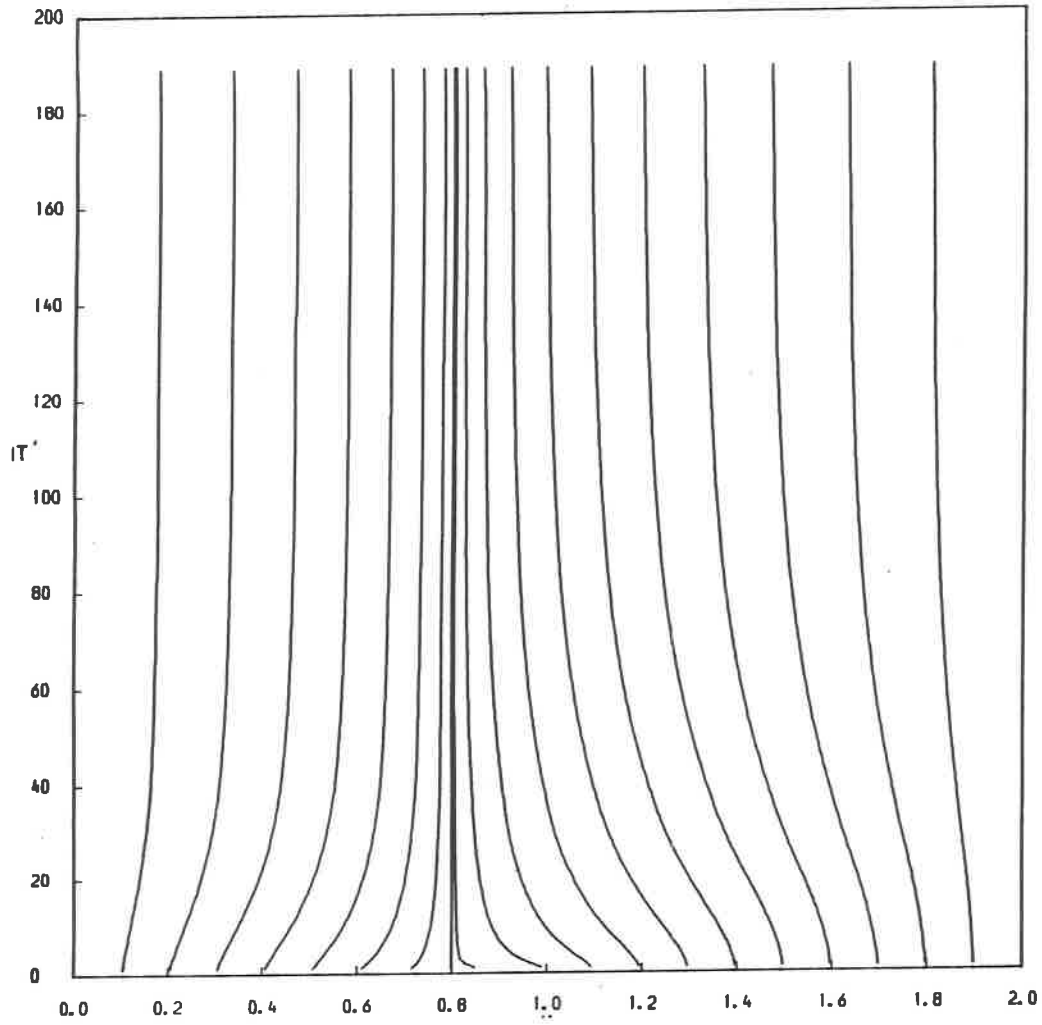

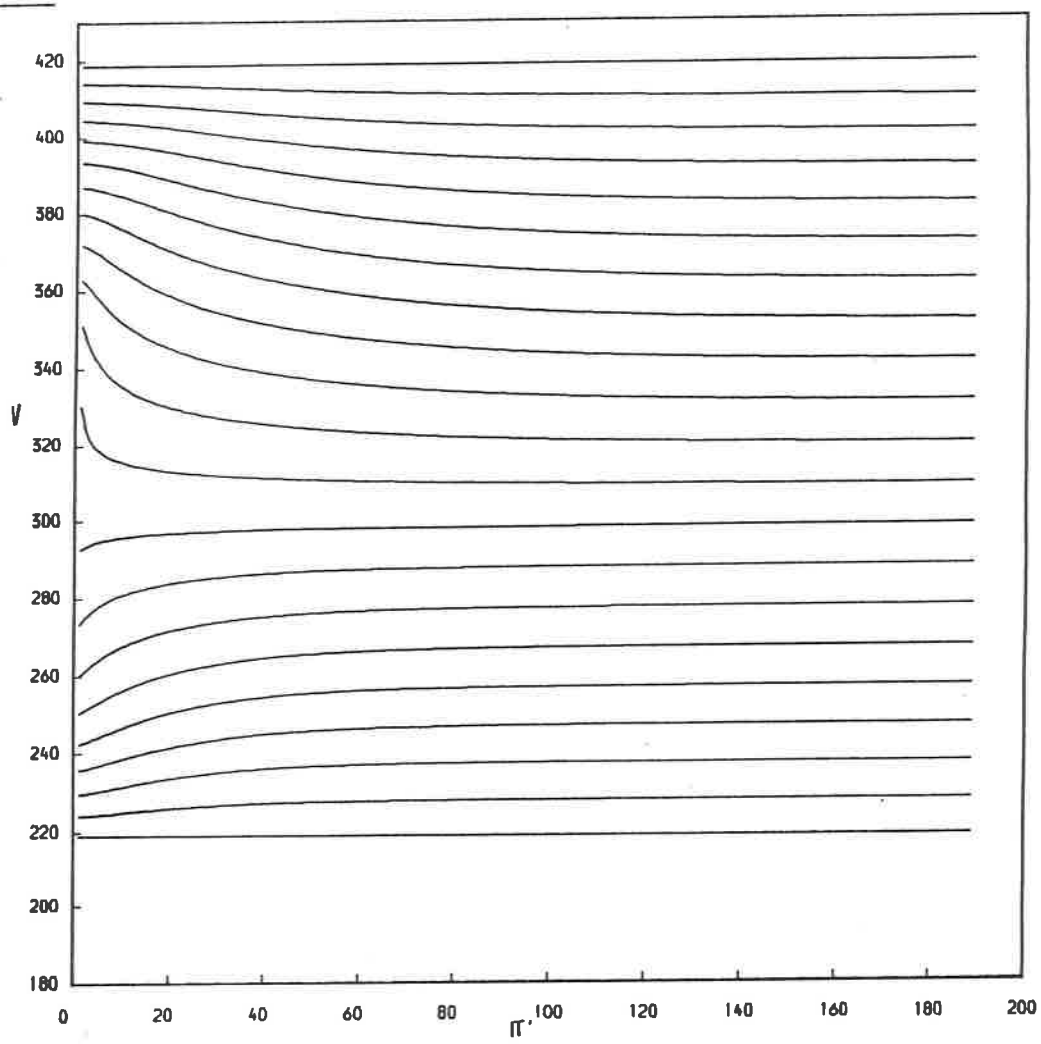

SUBSONIC FLOW
NODAL TRAJECTORIES
FIXED THROAT NODE
21 NODES

FIG. 20

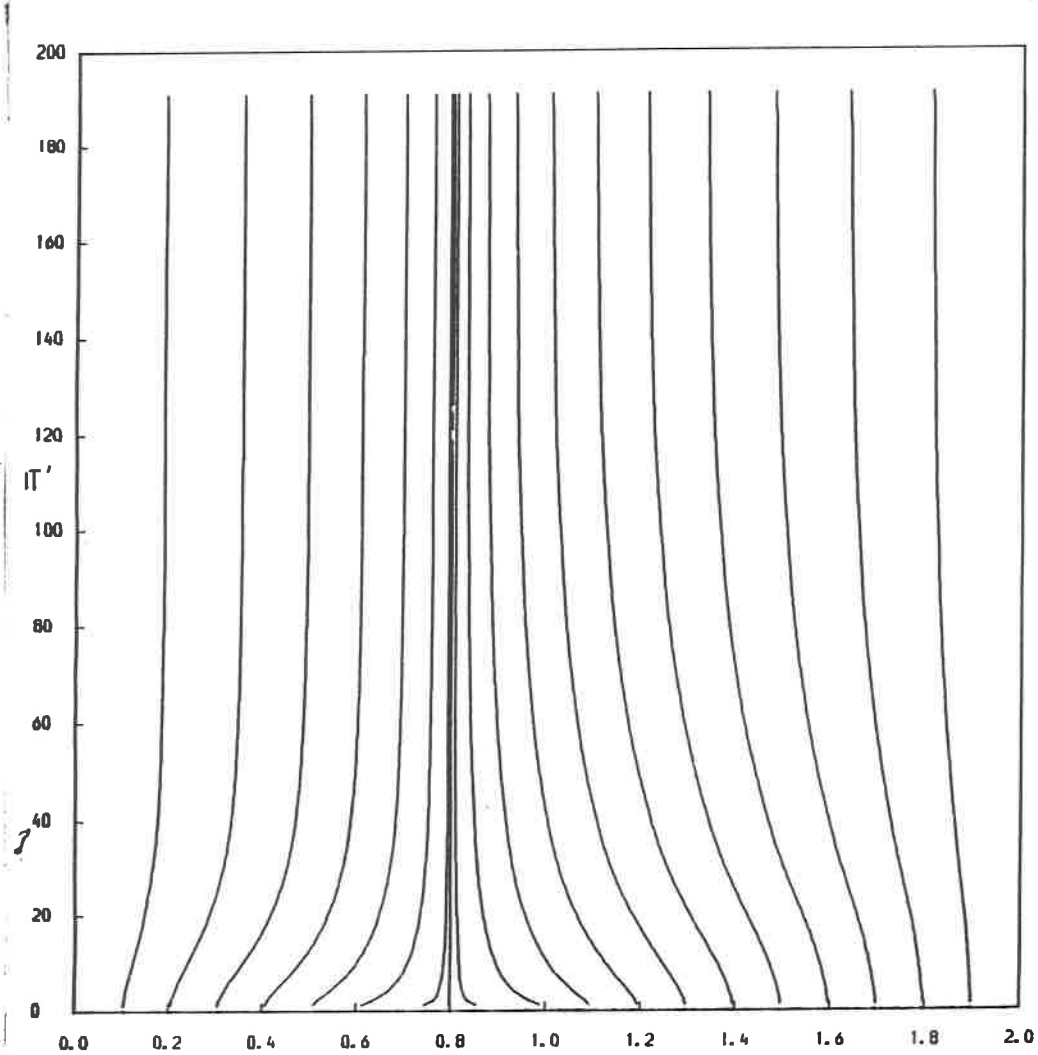

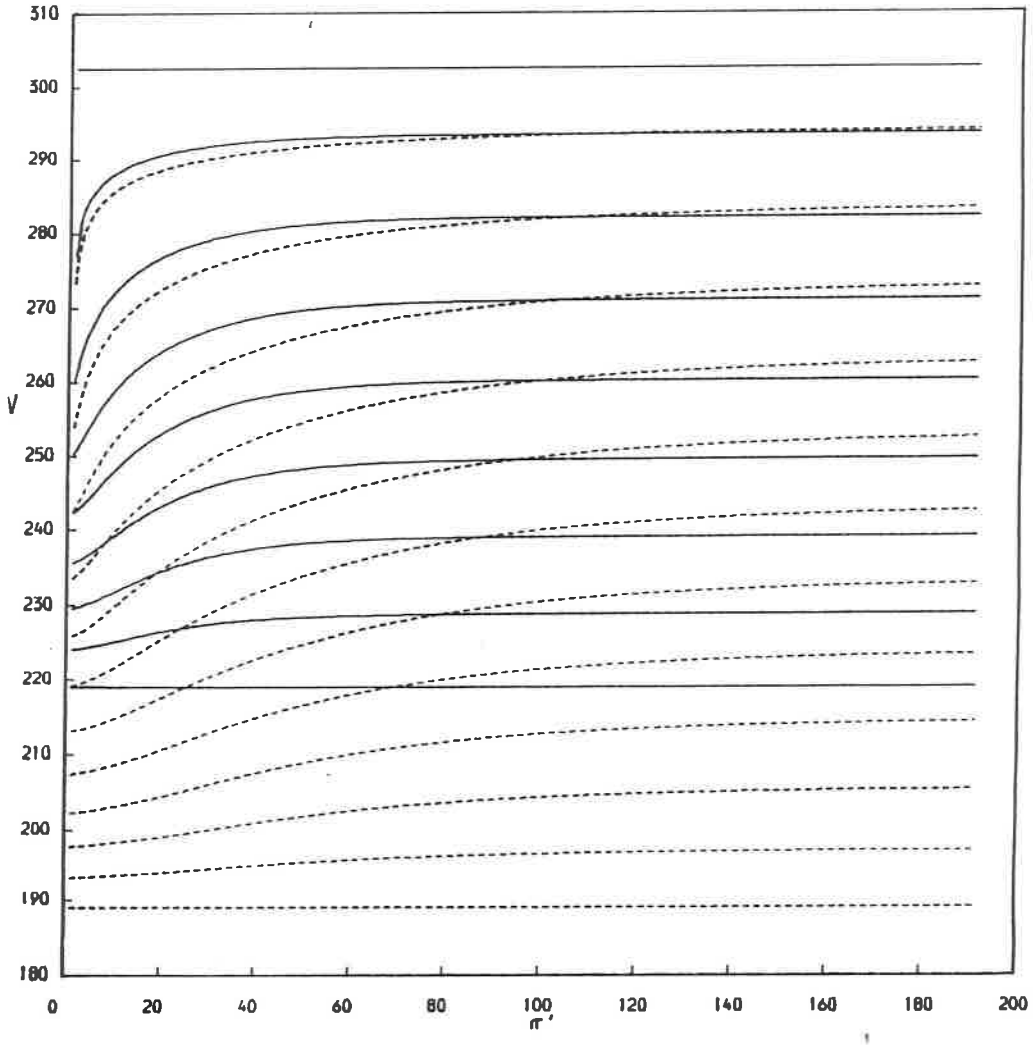

TRANSITION FLOW
NODAL TRAJECTORIES
FIXED THROAT NODE
21 NODES

FIG.21

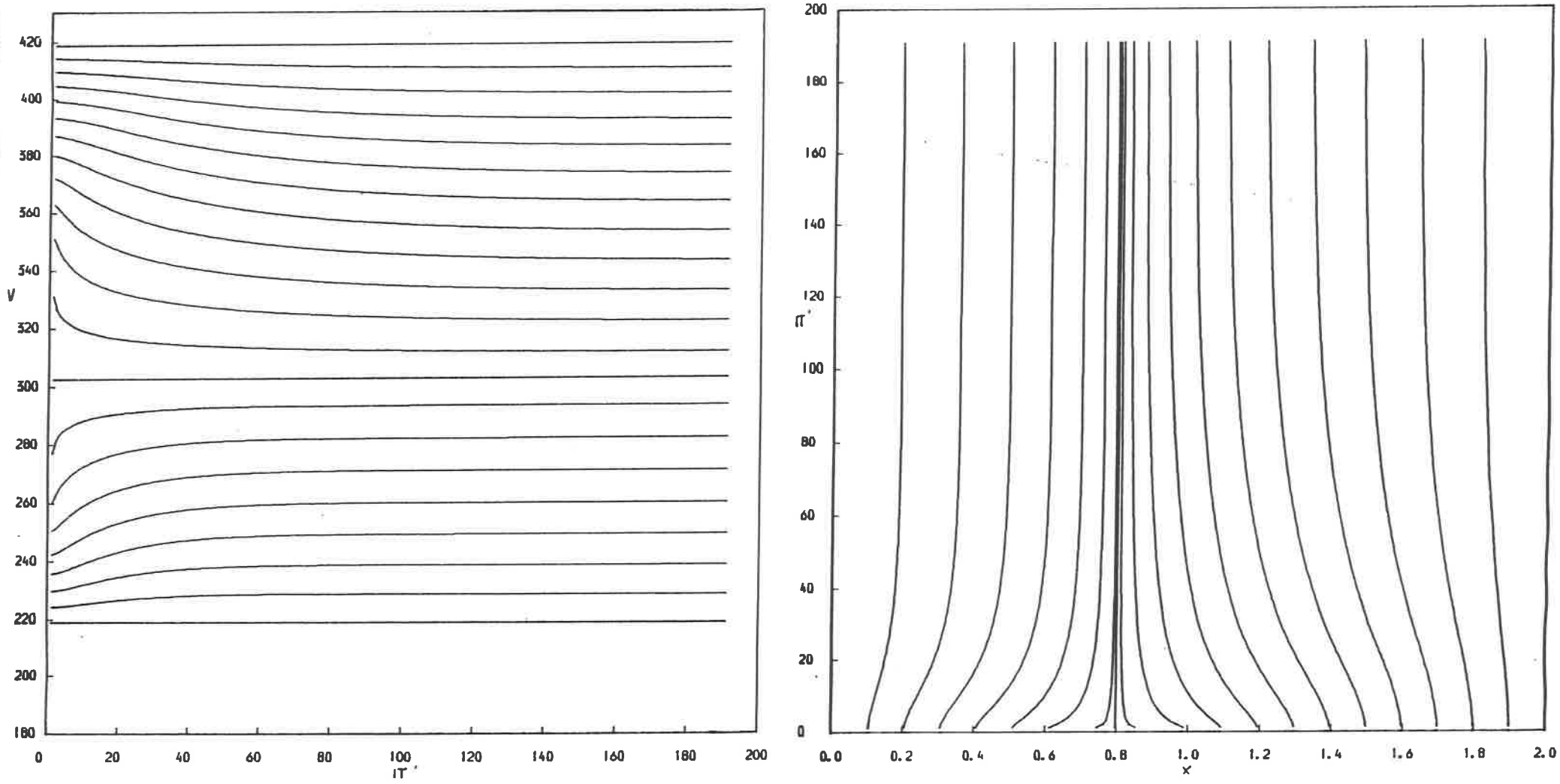

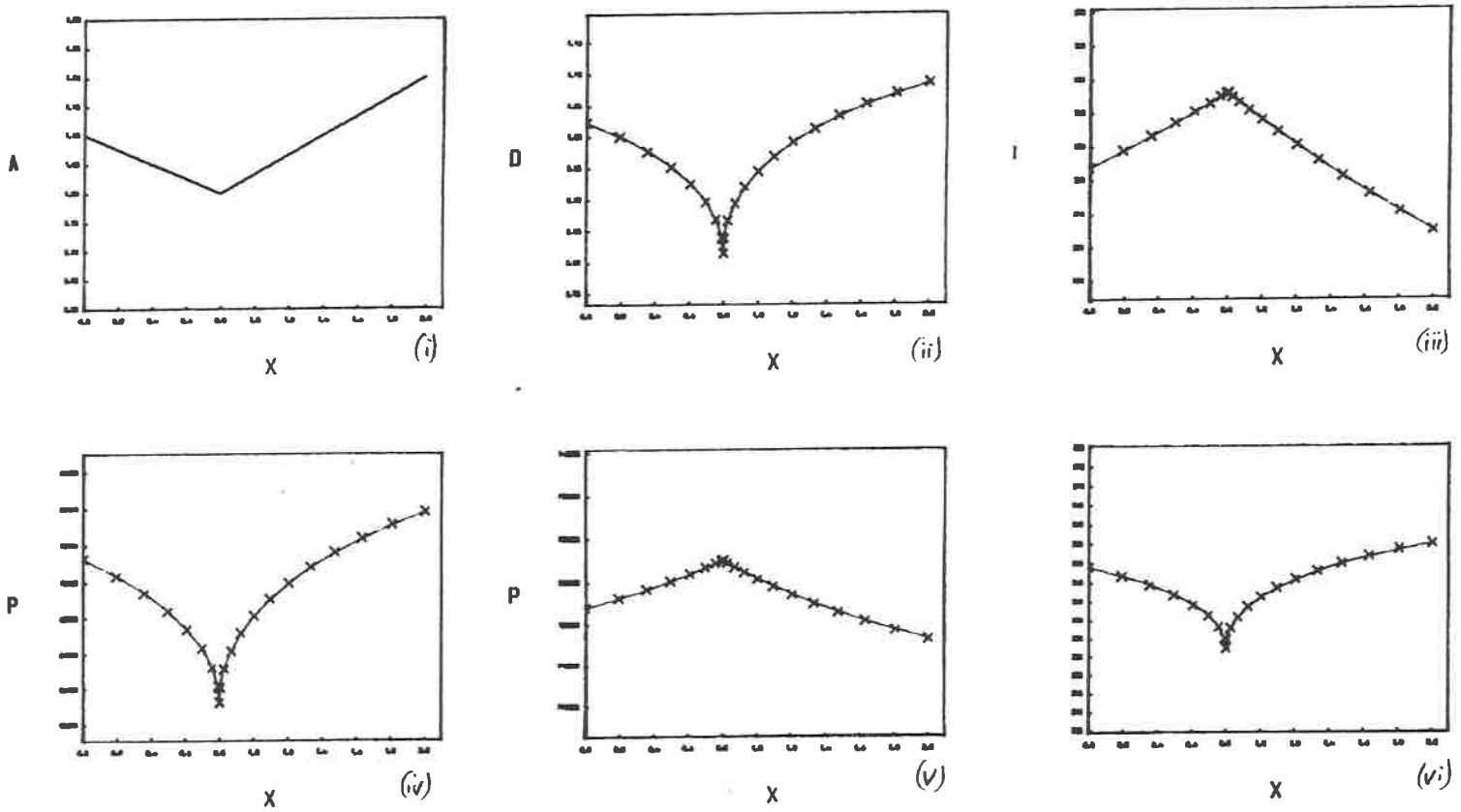

SUBSONIC FLOW
FLOW VARIABLE VARIATION
21 NODES

FIG. 22

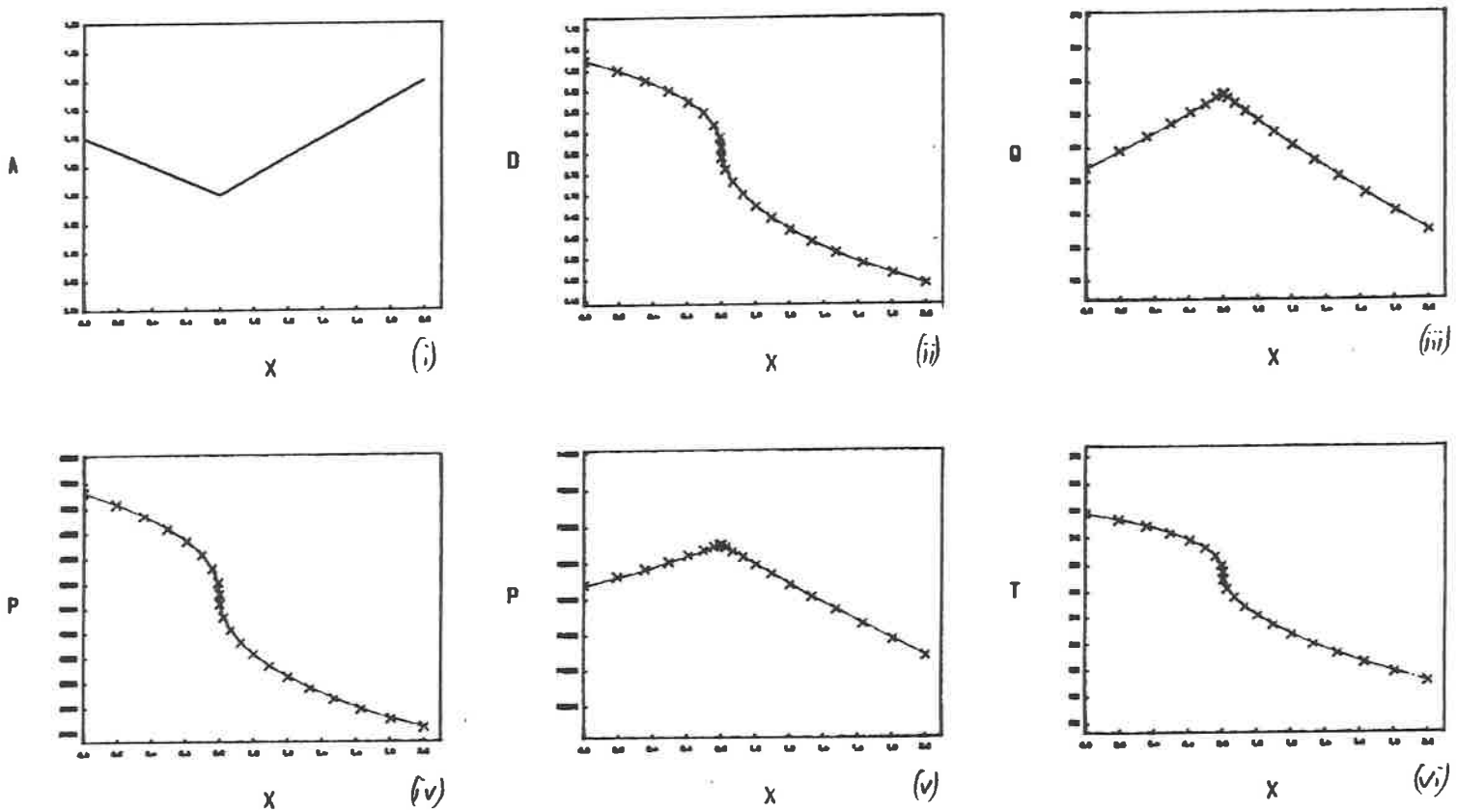

TRANSITION FLOW
FLOW VARIABLE VARIATION
21 NODES

FIG. 23

CONCLUSION

In this report a new method is presented which provides approximations to the flow variables in duct flow in terms of the distance along the duct axis. The method is novel in that it determines the grid at the same time as the approximate solution.

Finite element approximations are used for both aspects and a Jacobian iteration is employed to solve the non-linear normal equations involved. By manipulation of the equations a decoupling is obtained which allows sweeps of local updates, thus avoiding some of the ill-conditioning inherent in the Jacobian matrix.

An investigation is carried out into the efficiency of this procedure, including the effect of those nearly linear parts of the solution where unrealistically large co-ordinate updates are obtained.

REFERENCES

[1] WIXCEY, J.R. : "Compressible flow in ducts - analytic aspects", NUMER. ANAL. REPORT 12/88, DEPT. OF MATHS., UNIV. OF READING (1988).

[2] WIXCEY, J.R. : "Compressible flow in ducts - variational aspects", NUMER. ANAL. REPORT 13/88, DEPT. OF MATHS., UNIV. OF READING (1988).

[3] WATHEN, A.J. & BAINES, M.J. : "On the Structure of the Moving Finite-element Equations", I.M.A. J. NUM. ANAL. 5, (1982).

[4] SEWELL, M.J. : "Properties Of A Streamline In Gas Flow", PHYS. TECHNOL. 16, (1985).

[5] LOACH, P. : Private communication.